UNIVERSIDADE DE LISBOA
FACULDADE DE CIÊNCIAS
DEPARTAMENTO DE BIOLOGIA ANIMAL

Characterization of a new genetically modified *Plasmodium berghei* parasite – development of a pre-erythrocytic malaria vaccine

Mestrado em Biologia Humana e Ambiente

Carolina Morgado de Andrade

Dissertação orientada por:
Doutor António Mendes (Instituto de Medicina Molecular, Faculdade de Medicina, Universidade de Lisboa)
Prof.ª Doutora Deodália Dias (Faculdade de Ciências, Universidade de Lisboa)

2015

Dedico esta dissertação à minha família.
Por tudo o que sou hoje, devo-o a vocês.

This master thesis follows the citation format by *Nature*

Abstract

Malaria is an infectious disease caused by a protozoan parasite of the genus *Plasmodium* and transmitted to humans and other animals by infected female *Anopheles* mosquitoes. Although there are five species of *Plasmodium* that can infect humans, the majority of the deaths are caused by *P. falciparum* and *P. vivax*. Unfortunately, there is still no licensed vaccine against malaria.
Whole-organism pre-erythrocytic malaria vaccines have been shown to elicit sterile immunity in both humans and rodents. They induce effective $CD8^+$ T cell responses, required for sterilizing immunity in malaria. Nevertheless, current whole-organism pre-erythrocytic malaria vaccination approaches, which rely on the use of human-infective sporozoites, present risks and limitations that cannot be overlooked.
According to the 2013 World Health Organization guidelines, a malaria vaccine should be available for use and licensed by 2030, with at least 75% efficacy and capable of protecting against both *P. falciparum* and *P. vivax.*
Here, we propose a vaccination approach where a genetically modified rodent *P. berghei* parasite is used as a platform to deliver immunogenic antigens against the two major human infective *Plasmodium* species: *P. falciparum* and *P. vivax* – the *Pb*TriCS parasite. Our results show that *Pb*TriCS development during the sporogonic stage and *in vitro* hepatic stage is not impaired, having similar infectivity to wild-type parasites. Although our results in C57BL/6J mice have shown a reduced fitness by *Pb*TriCS parasites in establishing an *in vivo* liver infection, we demonstrated by ELISA assays that this parasite is able to trigger humoral responses against *P. falciparum* and *P. vivax* CS peptides.

We conclude that PbTriCS has the potential to be a good malaria vaccine candidate as it is able to elicit strong antibody responses against both *P. falciparum* and *P. vivax*. Further studies should be pursued to functionally demonstrate the protective capacity of the immune response induced through immunization with PbTriCS.

Keywords: Malaria vaccine, *P. berghei*, *P. falciparum*, *P. vivax*, circumsporozoite protein.

Resumo

A malária é uma doença infecciosa endémica em 97 países, causada por um protozoário do género *Plasmodium* e transmitida por um mosquito fêmea do género *Anopheles.* Existem cinco espécies capazes de causar infecção em seres humanos, *P. falciparum, P. vivax, P. malariae*, *P. ovale* e *P. knowlesi*. Destas, *P. falciparum* é o parasita predominante no continente africano e é o responsável pelo maior número de mortes. A Organização Mundial de Saúde (OMS) estima que em 2013 a malária foi responsável pela morte de 584 mil pessoas, sendo que destas, 453 mil correspondem a crianças abaixo dos cinco anos.[1 4 5]

O ciclo de vida do parasita da malária inicia-se quando um mosquito infectado se alimenta de sangue num hospedeiro humano, depositando na sua pele centenas de esporozoítos – a forma do parasita residente nas glândulas salivares do mosquito e capaz de infectar o fígado. Os esporozoítos entram rapidamente na circulação sanguínea chegando ao fígado, onde atravessam os sinusoides hepáticos e diversos hepatócitos, até invadirem um hepatócito com formação dum vacúolo parasitóforo, onde o parasita reside durante todo o seu desenvolvimento hepático[14]. A fase hepática da infeção por *Plasmodium* é uma etapa obrigatória do seu ciclo de vida, ainda que clinicamente silenciosa. No fígado, o parasita prolifera, diferenciando-se numa forma replicativa, a forma exo-eritrocítica. Em humanos, a infecção por *P. vivax* ou *P. ovale* pode dar origem a formas hepáticas dormentes, os hipnozoítos, que podem causar recaídas na doença, meses ou anos após a infecção.[4 5] A fase hepática termina com a libertação de vesículas cheias de merozoítos – os merosomas – para a corrente sanguínea.[16] Na corrente sanguínea os merosomas libertam os merozoítos que infectam os eritrócitos, iniciando assim o estádio eritrocítico da infeção. [4 16] Os merozoítos infetam os eritrócitos em ciclos de invasão, crescimento intracelular, multiplicação e re-infeção de novos eritrócitos.[18] As células-filhas dos merozoítos podem desenvolver-se em formas assexuadas ou sexuadas do parasita. As primeiras continuam o ciclo de invasão e multiplicação nos eritrócitos ao passo que as segundas originam gametócitos. É na fase sanguínea da infecção que a sintomatologia da malária aparece.[19 13] Aquando da ingestão de sangue por uma fêmea *Anopheles* num humano infectado, há a entrada de gametócitos presentes no sangue para o intestino médio do mosquito. Aqui, os gametócitos diferenciam-se em gâmetas, que se fundem, dando origem a um zigoto diplóide que inicia a meiose. Os zigotos transformam-se numa forma móvel, o oocineto que migra e penetra o epitélio do intestino médio do mosquito, onde se transforma numa forma séssil, o oócisto. O oócisto sofre replicação mitótica produzindo esporozoítos, que após a ruptura do oócisto ficam livres na hemolinfa indo invadir as glândulas salivares do mosquito. O parasita está então pronto para iniciar um novo ciclo num novo hospedeiro.[19]

Atualmente, as medidas de controlo de malária envolvem o controlo do vetor e o tratamento da doença. Infelizmente, não se encontra atualmente

licenciada nenhuma vacina contra a malaria, a qual será sempre uma ferramenta essencial para a erradicação desta doença. Em 2013 a OMS lançou orientações em relação ao desenvolvimento / licenciamento de uma vacina para a malária segundo as quais 2030 deverá haver uma vacina contra ambas as espécies *P. falciparum* e *P. vivax* e ter pelo 75% de eficácia.

Tradicionalmente, as estratégias de vacinação contra a malária incluem: as vacinas pré-eritrocíticas (têm como alvo o esporozoíto e a fase hepática da infeção); as vacinas eritrocíticas (têm como alvo a fase assexuada do parasita no sangue); e as vacinas que bloqueiam a transmissão (têm como alvo os gametócitos/gâmetas do parasita e/ou outros estádios no mosquito).[25] As vacinas pré-eritrocíticas são até ao momento as mais promissoras, podendo dividir-se em dois tipos: as de subunidade e as de organismo inteiro.

As vacinas de subunidade baseiam-se no uso de uma pequena porção do parasita, uma proteína ou um péptido, para evocar uma resposta imune. Por seu lado, as de organismo inteiro baseiam-se no uso do parasita todo, administrado numa forma atenuada, ou sob o tratamento com antimaláricos. Atualmente, o candidato a vacina mais avançado, e o único que chegou a estudos clínicos fase 3, é uma vacina de subunidade, a RTS,S, que usa a proteína *circumsporozoite* (CS) de *P. falciparum* para evocar respostas imunes.[32] No entanto, a sua eficácia é de cerca de 30% e diminui ao longo do tempo.[33]

As vacinas de organismo inteiro mostraram ser as mais eficazes visto que foi possível induzir respostas imunes em roedores e em humanos capazes de prevenir uma infecção subsequente por *Plasmodium.*[27 28 37] Além disso, as vacinas de organismo inteiro são capazes de espoletar respostas imunes mediadas por células T $CD8^+$.[38 39] No entanto, as vacinas de organismo inteiro apenas são contra uma espécie de *Plasmodium* e baseiam-se no uso de esporozoítos capazes de infetar humanos, o que representa riscos e limitações.

O PrudêncioLab do Instituto de Medicina Molecular, tem vindo a investigar o uso do *P. berghei* como uma estratégia de vacinação contra a malária. *P. berghei* é um dos parasitas de malária em roedores e em trabalhos anteriores ficou provada a sua capacidade de infectar células do fígado humano, bem como a sua incapacidade de se reproduzir em eritrócitos humanos, impedindo-o de causar a doença. Assim, *P. berghei* é uma abordagem de vacinação mais segura em relação a outros candidatos a vacina pré-eritrocítica de organismo inteiro. O PrudêncioLab caracterizou um *P. berghei* geneticamente modificado (GM) que expressa a proteína CS de *P. falciparum* sob o controlo do promotor UIS4 de *P. berghei*. Os resultados deste trabalho mostram que este parasita GM é capaz de suscitar uma resposta imune contra uma infeção causada por *P. falciparum.*

Tendo em conta as diretrizes da OMS, o PrudêncioLab criou recentemente um novo parasita *P. berghei* GM que expressa simultaneamente as proteínas CS de *P. falciparum* e *P. vivax* em *loci* neutros, o parasita *Pb*TriCS. Este projeto de mestrado teve como objetivo a caracterização deste parasita, avaliando a sua capacidade de desenvolvimento e infeção em mosquitos

Anopheles, in vitro em células Huh7, e *in vivo* em ratinhos C57BL/6J. Para concluir, avaliaram-se as respostas humorais contra péptidos das CS de *P. berghei, P. falciparum* e *P. vivax.* espoletadas pela imunização com *Pb*TriCS.

A primeira parte da caracterização consistiu em avaliar o desenvolvimento do parasita em mosquitos *Anopheles.* Para tal, contaram-se os números de oócistos no intestino médio e os números de esporozoítos presentes nas glândulas salivares. Comparados os resultados com os de *Pb*GIMO, a linha inicial não-transfetada e caracterizada como correspondendo ao *P. berghei* selvagem, não foram encontradas diferenças significativas entre parasitas, permitindo concluir então que a inserção de dois genes em *loci* neutros não tem impacto no desenvolvimento do parasita no mosquito. Procedemos então à análise do movimento de *gliding* dos esporozoítos numa superfície de vidro, não tendo sido encontradas diferenças significativas no número de círculos relativamente ao *Pb*GIMO e concluíndo também que as 3 CS são expressas no esporozoíto.

Na segunda parte do trabalho, caracterizámos o parasita *in vitro* através da infeção da linha celular de hepatoma humano Huh7. Concluímos, através da de microscopia de imunofluorescência, que *Pb*TriCS possui uma infetividade semelhante a *Pb*GIMO, sendo o seu desenvolvimento normal, às 48 após a infeção. Foi-nos possível também observar que todas as CS estão a ser corretamente expressas. Decidimos então avançar para a caracterização da infeção *in vivo* em ratinhos C57BL/6J às 46 horas após a infeção tendo-se observado por qRT-PCR uma redução na infeção do fígado por *Pb*TriCS comparativamente a *Pb*GIMO. A análise de secções de fígado por microscopia de imunofluorescência mostrou que esta redução de infeção se deve a um menor número de parasitas no fígado ao invés de um menor desenvolvimento dos mesmos. No entanto, todas as CS estão a ser corretamente expressas *in vivo* em *Pb*TriCS. Para entender esta observação, realizámos um ensaio de atravessamento celular, tendo-se concluído que o atravessamento por *Pb*TriCS é cerca de 50-60% inferior ao de parasitas *Pb*GIMO. Isto foi indiretamente confirmado pela observação experimental que o número de parasitas *Pb*TriCS capaz de estabelecer uma infeção no fígado de ratinhos C57BL/6J é menor que *Pb*GIMO.

Por último, na terceira parte do trabalho, utilizamos o parasita *Pb*TriCS para imunizar ratinhos C57BL/6J e, por ELISA, foi possível concluir que o soro dos ratinhos imunizados possui anticorpos capazes de reconhecer os péptidos das CS de *P. berghei, P. falciparum* e *P. vivax.*

Em conclusão, apesar do parasita *Pb*TriCS ter uma menor capacidade de estabelecer uma infeção hepática *in vivo* em comparação com *Pb*GIMO, os parasitas capazes de infetar o fígado não têm o seu desenvolvimento comprometido e expressam corretamente as várias proteínas CS, permitindo que uma imunização com *Pb*TriCS induza a produção de elevados títulos de anticorpos contra a CS de *P. falciparum* e *P. vivax*. Embora mais estudos devam ser feitos, nomeadamente ao nível de respostas imunes e de eficácia, podemos concluir que o parasita *Pb*TriCS constitui um bom candidato a vacina contra *P. falciparum* e *P. vivax.*

Palavras-chave: Vacina para a malária; *P. berghei*; *P. falciparum*; *P. vivax*; Proteína do *circumsporozoite*.

Acknowledgments / Agradecimentos

Quero começar por agradecer ao Miguel a oportunidade que me deu de desenvolver a minha dissertação de mestrado no PrudêncioLab. Acho que sempre deixei claro em todos os e-mails o quanto admirava (e admiro ainda mais) o projeto e a motivação que tinha em fazer a tese no teu laboratório. Permitiste-me concretizar um sonho ao aceitares-me como estudante de mestrado. Foi um ano incrível, em que aprendi mais do que poderia antecipar, e tudo se deve a teres-me aceitado no teu laboratório. Nunca conseguirei expressar o quão grata me sinto.

Ao António, por ter sido o melhor orientador que poderia ter tido. Pela autonomia que cedo me incutiste, responsabilizando-me na independência que tive nas experiências e, ao mesmo tempo, me ensinares tanto. Agradeço-te por teres puxado imenso por mim e nunca duvidares das minhas capacidades, mesmo quando eu duvidava. Obrigada!

À Prof.ª Deodália, por me ter incentivado, conduzindo-me à frequência deste mestrado, pela dedicação aos seus alunos e pelo carinho. Um obrigada pela paciência e um pedido de desculpa pelas visitas frequentes ao seu gabinete num "verdadeiro estado de nervos". Obrigada!

A todos os membros do laboratório, por fazerem do PrudêncioLab o laboratório mais espetacular do IMM! Quero agradecer pela paciência, pelos conselhos, pelo carinho com que me acolheram e alcunha carinhosa que me puseram. Ao Jorge, por me ter feito questionar tudo e ensinar a ser minuciosa em relação às minhas experiências. Admiro-te como cientista e desejo-te a maior sorte nesta nova fase da tua vida. Não tenho dúvidas que serás incrível! À Marta, por tanto que não seria possível enumerar aqui. És uma pessoa com uma energia incrível e contagiante. Obrigada por todo o apoio! À Patrícia - embora o negues, és das pessoas mais genuinamente boas que conheço! Obrigada por teres sempre uma palavra e um abraço querido. À Filipa, um pedido de desculpa pelas perguntas parvas e um obrigada por tornares aquele laboratório numa animação e alegria constantes. À Margarida, por todo o carinho, simpatia e palavras amigas. To Marija, thank you for keeping me company in all the late night experiments and the advices you gave me when I arrived that I will never forget. Good luck in this new adventure! À Joana, não só por teres criado o nosso parasita mas também pelos conselhos que me deste e por me teres ensinado muito nos primeiros dias de laboratório. Boa sorte no teu doutoramento, estou certa que serás brilhante! Ao Miguel Duarte, obrigada pelos conselhos, por me ensinares e desejares o melhor durante este ano. Não foi fácil seguir-te como estudante de mestrado do PrudêncioLab. Aos novos estudantes do PrudêncioLab, Raquel e João, que em tão pouco tempo já tenho muito a agradecer pela boa disposição e palavras de incentivo, na fase final e mais exigente deste projeto. Desejo-vos muito boa sorte neste ano. Vai ser um ano incrível e não podiam estar melhor entregues!

Também gostaria de agradecer ao FigueiredoLab por serem uns vizinhos impecáveis e, em especial, ao Francisco, à Leonor, ao Fabien e ao Fábio Bento por todos os conselhos, sugestões, dicas, motivação, etc. Obrigada! Por último, e não menos importante, ao MotaLab em especial à Ana, à Margarida, ao João, to Aparajita and Debanjan for being always available to questions and support. A huge thank you!

À minha família, por todo o apoio incrível que me deram ao longo dos meus 25 anos. Por nunca terem duvidado de mim e sempre me apoiarem em tudo, por terem ficado tão ou mais felizes que eu em ter conseguido fazer a tese no laboratório que mais desejava. Aos meus pais, pela minha educação, pelas boleias tardias neste ano, pela ética na vida e no trabalho, que aprendi convosco, e por tudo. Ao Leonardo, à Rita e à Gisela por serem os melhores irmãos que é possível ter. To Jacinta for all the advices concerning investigation. Ao Carlos, por seres o único leigo, além do Leo, que percebe muito razoavelmente o que aqui está escrito e por todos os conselhos que me deste ao longo da minha vida académica. E ao Nuno, por todo o interesse, paciência e carinho. Tudo o que sou hoje devo-o a vós. E quem me conhece sabe o orgulho que tenho na minha família. Obrigada por tudo.

Aos meus amigos por todo o apoio e por serem o meu porto de abrigo.

Ao Bernardo, por tudo. Por me teres dado espaço para me dedicar à tese, por me ajudares nos momentos mais difíceis. Por acreditares em mim e estares sempre ao meu lado. Obrigada.

A todos os que não estão aqui mencionados, mas que me ajudaram e apoiaram nesta fase, seja com um sorriso ou uma palavra amiga, obrigada.

INDEX

LIST OF FIGURES

LIST OF TABLES

ABBREVIATIONS

2346	PbTriCS motherline	**kb**	Kilo Base Pairs
5-FC	5-fluorocytosine	**p.i.**	post-infection
bp	Base Pairs	***Pb*CS**	*Plasmodium berghei* Circumsporozoite Protein
BSA	Bovine Serum Albumin	**PBS**	Phosphate-Buffered Saline Solution
cDNA	Complementary Deoxyribonucleic acid	**PCR**	Polymerase Chain Reaction
CS	Circumsporozoite	***Pf*CS**	*Plasmodium falciparum* Circumsporozoite Protein
DNA	Deoxyribonucleic acid	***Pv*CS**	*Plasmodium vivax* Circumsporozoite Protein
dNTP	Deoxyribonucleotide triphosphate	**qRT-PCR**	Quantitative Real-Time Polymerase Chain Reaction
EEF	Exo-Erythrocytic Form	**RAS**	Radiation Attenuated Sporozoites
FACS	Fluorescence-Activated Cell Sorting	**RBC**	Red Blood Cell
GAP	Genetically Attenuated Parasites	**RNA**	Ribonucleic Acid
GOI	Gene of Interest	**RPM**	Rotations per Minute
hdhfr	*human dihydrofolate reductase*	**RPMI**	Roswell Park Memorial Institute medium
HEPES	4-(2-hydroxyethyl)-1-piperazineethanesulfonic acid	**SM**	Selectable Marker
HPRT	Hypoxanthine Guanine Phosphoribosyl Transferase	**TR**	Targeting Region
Huh7	Human Hepato Cellular Carcinoma Cells	**UTR**	Untranslated Region
i.p.	Intraperitoneal Injection	**WT**	Wild-Type
i.v.	Intravenous Injection	***yfcu***	yeast *cytosine deaminase* and *uridyl phosphoribosyl transferase*

INTRODUCTION

1

1. INTRODUCTION

1.1 Malaria: Key facts

Malaria is a mosquito-borne disease, which is endemic in 97 countries, affecting 3.3 billion people, 1.2 billion of whom are at high risk of contracting malaria.[1] The World Health Organization estimated 198 million cases of malaria in 2013 (95% uncertainty interval, 124-283 million), 584 thousand of which resulted in death (95% uncertainty interval, 367-755 thousand), including 453 thousand deaths of children under the age of five.[1] Malaria has high rates of mortality as well as morbidity, affecting the economy of endemic regions, where malaria and poverty are closely related, making this disease a major obstacle to the economic development of affected regions.[2 3]

Malaria is caused by an apicomplexa parasite of the genus *Plasmodium,* which is transmitted by female mosquitoes of the genus *Anopheles*, the definitive host of *Plasmodium,* where sexual reproduction takes place.[4] There are five species of *Plasmodium* that may cause the disease in humans: *P. falciparum*, *P. vivax*, *P. malariae*, *P. ovale* and *P. knowlesi*. *P. falciparum* and *P. vivax* are the most common.[4] The former may lead to cerebral malaria and is responsible for the majority of the cases of malaria-associated death. The latter not only is responsible for 47% of malaria cases outside the African continent, but it may also form dormant parasites, termed hyponozoites, which may cause disease relapses. [1 5]

1.2 Epidemiology

P. falciparum and *P. vivax* represent the greatest malaria-related public health concerns since they are responsible for the highest incidence rates.[1]

Although *P. falciparum* is responsible for the majority of deaths, it is predominant mostly in the African continent whereas *P. vivax* is more widespread since this species can develop in its vector can endure higher altitudes and cooler climates.[1] Despite *P. vivax* being more widespread than *P. falciparum*, it has a lower transmission due to the predominance of the Duffy-negative genotype among the African continent.[1] (Figure 1) *P. vivax* was thought to require the Duffy antigen to invade human erythrocytes, and in its absence, invasion is prevented. [6 7 8] However, recent studies have described *P. vivax* infection in Duffy negative individuals.[9] There are 3 alleles that characterize the Duffy blood group: FYA, FYB and FYO and four different phenotypes: Fy (a+ b+), Fy (a+ b-), Fy (a- b+) and Fy (a- b-). The latter is predominant in African populations and individuals carrying this phenotype are resistant to a *P. vivax* infection. [10 11]

Other genetic traits are known to provide protection and genetic resistance to malaria infection, such as sickle-cell anemia, thalassemia, hemoglobinophaties, glucose-6-phosphate dehydrogenase (G6PD) deficiency and O allele from the ABO blood group. [12]

Malaria-associated symptoms can vary between mild and severe: the symptoms begin with fever, headache, fatigue, muscle aches, nausea, vomiting, anemia and a palpable spleen a few days after the start of the disease. In children, a palpable liver is present whereas jaundice is notable in adults. The disease may progress to severe malaria where the symptoms include acute pulmonary edema and kidney injury, generalized seizures and coma and if not treated, death. [13] For a long period of time, it was believed that an infection with *P. vivax* was benign and was not responsible for the same numbers of mortality as *P. falciparum*. However, recent reports have shown that *P. vivax* infection is able to cause severe malaria, respiratory distress and coma, and has similar mortality rates to *P. falciparum.* [7 14]

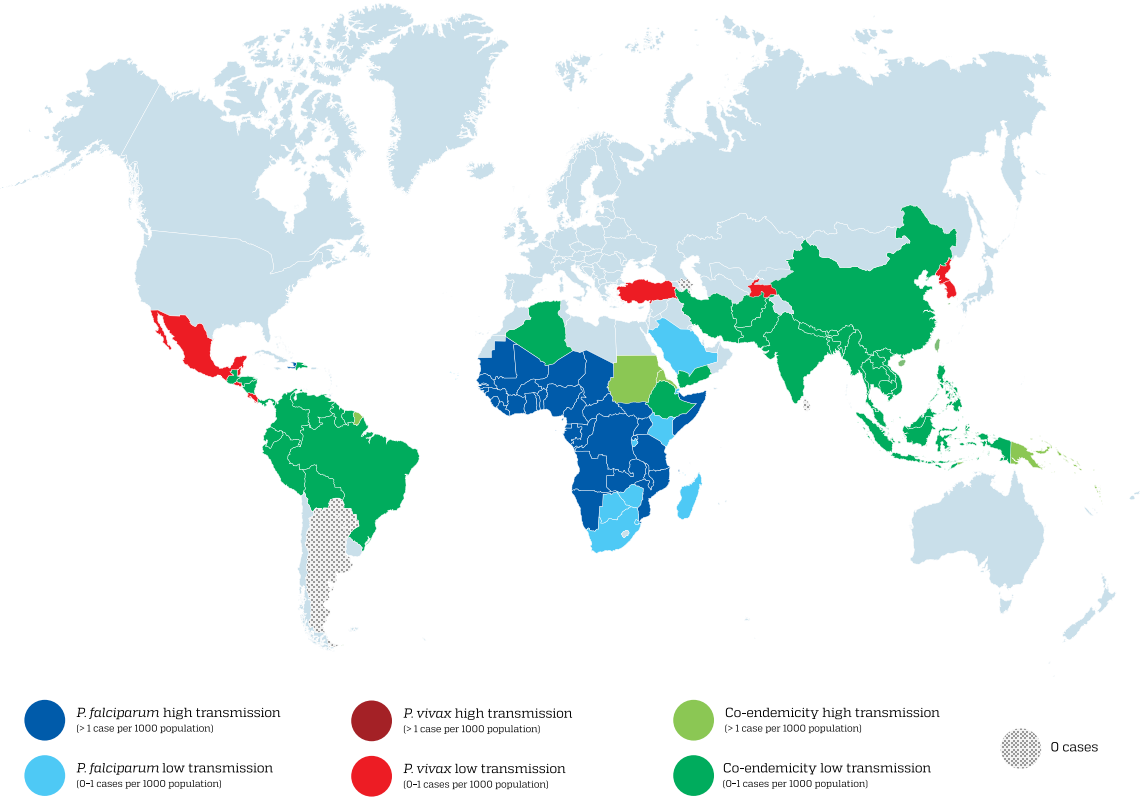

Figure 1: Transmission of *P. falciparum, P. vivax* and co-endemicity of *P. falciparum* and *P. vivax* worldwide between high and low transmission.
Map created using World Health Organization Malaria Report 2014 based on individual country profiles. [1]

1.3 *Plasmodium* life cycle

The life cycle of *Plasmodium* (Figure 2) parasite begins when an infected female *Anopheles* mosquito takes a blood meal injecting hundreds of sporozoites into the skin of the mammalian host. Sporozoites, the liver-infective forms of *Plasmodium* parasites that reside in the mosquito's salivary glands, eventually reach a blood vessel through a mode of locomotion known as gliding motility. After entering the bloodstream, the sporozoites reach the liver within minutes where they cross the liver sinusoids (fenestrated blood

vessels lined with endothelium and Kupffer cells), and traverse several hepatocytes by a process of migration known as cell traversal where they disrupt the hepatocytes plasma membrane without invading them. [15] Ultimately, sporozoites productively invade a hepatocyte with the formation of a parasitophorous vacuole (PV) where the parasite will reside during its liver stage development. The PV membrane (PVM) is the main interface between the parasite and the host. Inside the PV the parasite proliferates and dedifferentiates into a replicative form, the exo-erythrocytic form (EEF). Infection by human parasites *P. vivax* and *P. ovale* may produce cryptic liver-stage forms, known as hypnozoites, that can stay dormant for months or even years, before resuming development, eventually causing disease relapses.[4 5]

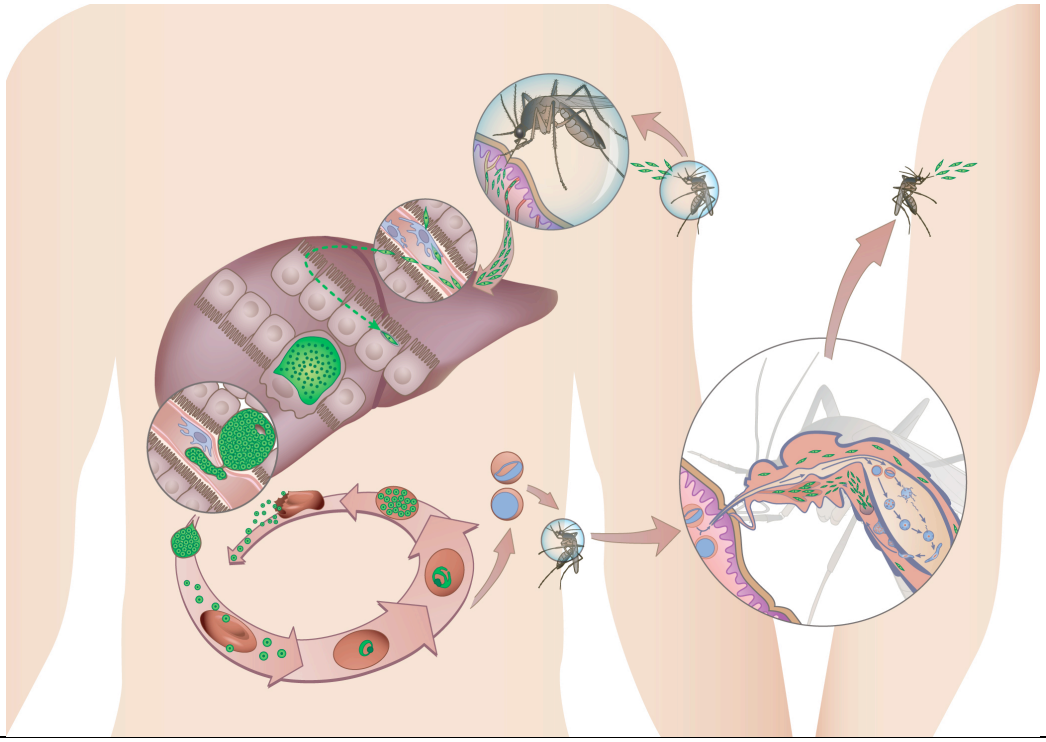

Figure 2: Life-cycle of the *Plasmodium* parasite.
Parasite transmission occurs when an infected female *Anopheles* mosquito takes a blood meal on a susceptible vertebrate host. The mosquito injects sporozoites into the skin, which enter the blood stream eventually reaching the liver. In the liver, sporozoites traverse several hepatocytes until infecting one. *P. vivax* and *P. ovale* may develop into dormant forms, the hypnozoites. The liver stage of infection ends with the release of merozoites that invade erythrocytes initiating the blood stage of infection and causing malaria symptoms. *Plasmodium* differentiates into gametocytes, male (microgamete) and female (macrogamete) and the mosquito upon a blood meal ingests them. In the mosquito's midgut, microgametes penetrate the macrogametes generating zygotes. The zygotes become motile and elongated and are called ookinetes. These penetrate the mosquito's midgut wall and will develop into oocysts. The oocysts mature and sporozoites develop within. Upon oocysts rupture, they release sporozoites that will migrate to the mosquito's salivary glands. Upon the mosquito's next blood meal, sporozoites are injected into the host's skin and the cycle continues.

The EEF enters schizogony, undergoing rapid growth, where the parasite exceeds the size of an uninfected hepatocyte by 10 times,[16] and DNA

replication. The liver stage of infection is a clinically silent to the host, yet obligatory, step in the lifecycle of the parasite, and culminates with the release of merozoite-filled vesicles, the merosomes, into the bloodstream. It is estimated that each merosome packs up from a few to thousands of merozoites. [16] In the bloodstream, the merosomes eventually burst in the microvasculature of the lungs, [17] releasing the merozoites, *Plasmodium* erythrocyte-infective forms, which will then initiate the blood stage infection. The liver stage of *Plasmodium* infection requires distinct time for each developmental stage in rodent and human malaria. The full liver stage infection takes 5 to 15 days for human-infective *Plasmodium* species, whereas in parasites infecting rodent hosts the parasite only takes 2 days to complete the process. [4] [16].

Once in the blood, the parasite undergoes successive cycles of invasion, intracellular growth, multiplication and re-invasion, beginning with merozoites invading erythrocytes (red blood cells – RBC) by attaching to their surface, entering and enclosing themselves inside. Inside the RBCs, the parasite acquires a biconcave disc form known as ring stage. The parasite then rounds up and becomes a trophozoite, actively feeding, growing and modifying the RBC. The next parasite form is the schizont, where the parasite nucleus will divide to form approximately 16 nuclei. Merozoites then become visible at the RBC periphery, each one containing a nucleus. The blood stage cycle may start all over again when the RBC breaks down and the merozoites are released into the bloodstream. [18] These daughter merozoites from individual schizonts develop into either asexual stage or sexual stage parasites. The former will continue the cycle by invading new RBCs whereas the latter originate microgametocytes (males) or macrogametocytes (females). Gametocyte development starts identically to the asexual erythrocytic cycle, as the sexually committed merozoite invades a new RBC and grows into a trophozoite, later transforming into gametocytes instead of developing into schizonts. [19] It is in the blood stage of infection that the malaria-associated symptoms appear. [13]

Gametocytes and erythrocytic parasite stages are ingested when a female *Anopheles* mosquito takes a blood meal from an infected host. The ingested blood will go to the mosquito midgut lumen where mosquito-specific factors and environmental factors will trigger parasite gametogenesis, transforming gametocytes into extracellular gametes. Microgametocytes undergo three mitotic replication producing eight daughter genomes by a process called exflagellation, where the motile microgametes fertilize the macrogametes that have already emerged from the host erythrocyte. Fusion of the micro and macrogametes forms diploid zygotes that initiate meiosis without nuclear or cellular division. Zygotes then transform into a motile-form called ookinete that will migrate and penetrate the midgut epithelium shifting from the lumen to the midgut basal lamina, where it transforms into a sessile spherical form, the oocyst. After the oocyst is formed, mitotic replication begins and continues throughout the period of sporogony that occurs within the oocyst, resulting in $1x10^3$ to $1x10^4$ sporozoites being produced by oocyst. During this period, the oocyst increases in size and eventually the oocyst capsule starts to fragment and small holes appear through which sporozoites escape leaving the

collapsed oocyst capsule on the external surface of the midgut. Sporozoites are then free in the mosquito haemolymph where some, but not all, will successfully invade the mosquito's salivary glands by gliding motility with the formation of a parasitophorous vacuole [19].

1.4 Malaria control measures

Since there is still no licensed vaccine for malaria, the control of *Plasmodium* populations relies on the control of its vector *Anopheles spp.* Vector control measures include insecticide-treated nets (ITNs) and indoor residual spraying (IRS). [20] Although these measures were able to protect the population at risk of contracting malaria, insecticide resistance is spreading. [1] This is of great concern since it may lead to resurgence of malaria in non-immune populations, leading to an increase in mortality and morbidity. [21]

The World Health Organization (WHO) recommends the use of Artemisinin-based Combination Therapies (ACTs) for the treatment of *P. falciparum* and *P. vivax*. In areas where there is no documented resistance to chloroquine this should be used for the treatment of *P. vivax.* Artemisinin-based monotherapy should be avoided since it leads to parasite resistance against artemisinin. [1] Currently, the only drug available against dormant liver-stage hypnozoites is primaquine, which can prevent relapses in *P. vivax* and *P. ovale* infections. However, primaquine can lead to acute haemolytic anemia in G6PD-deficient individuals. [22]

Throughout history, eradication programs that relied mostly in vector control have proven to be inefficient, such those against malaria and yellow fever. On the other hand, eradication campaigns based on vaccination successfully eradicated smallpox globally and eradicated polio in some regions. [23]

1.5 WHO Malaria Vaccine Technology Roadmap

In 2013, the WHO issued some guidelines in the Malaria Vaccine Technology Roadmap concerning the licensing of malaria vaccines.

As stated: [24] By 2030, license vaccines targeting *Plasmodium falciparum* and *Plasmodium vivax* that encompass the following two objectives, for use by the international public health community:

- Development of malaria vaccines with protective efficacy of at least 75 percent against clinical malaria suitable for administration to appropriate at-risk groups in malaria- endemic areas.

- Development of malaria vaccines that reduce transmission of the parasite and thereby substantially reduce the incidence of human malaria infection. This will enable elimination in multiple settings. Vaccines to reduce transmission should be suitable for administration in mass campaigns.

1.6 Malaria Vaccines

Naturally acquired immunity (NAI) against blood stage malaria occurs in individuals in endemic areas and protects them from severe disease and death when exposed to *Plasmodium.* [25] In areas where malaria is hyper and holoendemic, meaning that transmission is high and near every individual is infected, NAI provides protection to adults and older children from severe mortality and morbidity, as the disease becomes asymptomatic in these individuals, but little is known about how this protection occurs. [26] Although an asymptomatic status is achieved among adults, sterile immunity against infection is never accomplished. [26]

Studies in the late 1960s by Nussenzweig *et al.* showed that radiation attenuated sporozoites could induce protective immunity to infection in mice.[27] In the early 1970s, Clyde *et al.* showed that immunization of naïve volunteers with irradiated *P. falciparum* sporozoites led to high levels of immunity. [28] This work was the first proof that the development of a vaccine is indeed possible and that the scientific community should continue to focus on the search for a suitable malaria vaccine. [29]

Traditionally, there are three *Plasmodium* vaccination approaches that depend on the lifecycle stage that is the target for the host's immune response. These include pre-erythrocytic malaria vaccines, which target the sporozoite and liver stage prior to blood infection; erythrocytic malaria vaccines, which target the asexual blood stage of the parasite; and transmission-blocking malaria vaccines, which target the gametocyte/gamete stage of the parasite, thus blocking transmission between the host and the mosquito. [25]

- Pre-erythrocytic vaccines, if proven efficacious, should not only prevent disease by preventing blood infection but also block the transmission to the mosquito. [29] Additionally, the pre-erythrocytic stage is ideal for vaccination since only a small number of sporozoites are injected by the mosquito, in contrast with thousands of merozoites that are released into the blood. Due to the clinically silent nature of the pre-erythrocytic stage of the parasite lifecycle, this is an excellent target to elicit immune responses. [30]

- Erythrocytic vaccines, although targeting the asexual blood stages of the parasite, do not prevent infection, instead reducing clinical symptoms or severe illness. [29] The most advanced erythrocytic vaccine candidates target antigens that coat the surface of merozoites or antigens involved in invasion of erythrocytes. [29] Examples of these candidates include $MSP1_{19}$ that targets the merozoite surface protein 1 (MSP1) therefore inhibiting erythrocyte invasion and AMA1, apical membrane antigen 1, which is thought to prevent erythrocyte invasion and is shown to inhibit erythrocyte invasion *in vitro* and it may also impair hepatocyte invasion. Studies and trials with these vaccine candidates have shown discouraging results in pursuing erythrocytic vaccines against malaria. [29]

- Transmission-blocking vaccines are based on antibodies that target antigens unique to gametocytes or gametes in order to interrupt development of the parasite in the mosquito, therefore blocking transmission from the host to the mosquito. [29] There are some transmission-blocking vaccines that advanced into clinical trials, namely Pfs25 for *P. falciparum* and Pvs25 for *P. vivax*. These vaccines target a protein expressed on the surface of the zygote and the ookinete. [25] These vaccines are thought of as "altruistic vaccines" [25] because the vaccinated individuals are not protected from infection nor disease. [29] Thus, in order to specify the efficacy of such vaccine candidate, an entire community must be vaccinated to determine if transmission of the parasite wears down. [25]

A desirable vaccine candidate should produce protective immune responses that outweigh the responses in naturally acquired immunity to malaria. Not only should these immune responses act rapidly, but they should also be long lasting and entirely prevent infection. [29] This thesis will present some more extended information on pre-erythrocytic malaria vaccines as they are the main focus of the thesis work.

1.6.1. Pre-erythrocytic malaria vaccines

As mentioned above, in the early 1970s Clyde *et al.* have shown the potential of a pre-erythrocytic vaccine to produce sterile immunity in naïve volunteers against *P. falciparum*, making the pre-erythrocytic stage the only stage demonstrated to be capable of eliciting sterilizing immunity. [31]

Pre-erythrocytic malaria vaccines can be divided into two groups, depending on the strategy employed to elicit the immune responses: sub-unit and whole-organism vaccines.

1.6.1.1. Sub-unit pre-erythrocytic malaria vaccines

Pre-erythrocytic subunit malaria vaccines use a small portion of the parasite, usually a protein or a peptide, as the antigenic basis to elicit an immune response whereas pre-erythrocytic whole-organism malaria vaccine uses the whole parasite, either attenuated or under antimalarial therapy.

Concerning the sub-unit malaria vaccines, RTS,S/AS01, created in 1987, is the most advanced malaria vaccine candidate to date and the first malaria vaccine candidate to undergo large-scale phase 3 clinical trials in Africa. [32] RTS,S/AS01 targets the pre-erythrocytic stage of *P. falciparum* eliciting antibody responses to its circumsporozoite (CS) protein.[32] RTS,S/AS01 is composed of the *P. falciparum* CS protein central repeat region (R) and T cell epitopes (T) fused with hepatitis B surface antigen (S) and co-expressed in *Saccharomyces cerevisiae* (S) (Figure 3). RTS,S is formulated with AS01 adjuvant to enhance immune response to antigens and previous studies have confirmed that RTS,S/AS01 is able to provide protective immunity. [29 31 33]

Final results from phase 3 clinical trials were published in July 2015 and reported on the efficacy and safety of the vaccine 3 years after first

vaccination. The study was designed such that young infants (6-12 weeks old) and children (5-7 months old) received three doses of the vaccine at months 0, 1 and 2, and a booster dose, or not, at month 20. Concerning young infants who received the booster dose, vaccine efficacy is 26% and 17% against clinical and severe malaria, respectively. For infants who did not received the booster dose, vaccine efficacy decreased to 18% regarding clinical malaria and 10% for severe malaria. As for children that received the four doses, vaccine efficacy was 36% and 32% against clinical and severe malaria, respectively. For children who did not received the booster dose, vaccine efficacy decreased to 28% against clinical malaria and to 1% against severe malaria. [33] Studies also report that RTS,S vaccine efficacy wanes over time and children who do not receive a booster dose of vaccination are more prone to develop severe malaria. Authors hypothesize that this might be a result of loss of naturally acquired immunity to malaria due to vaccination.[32] [33] RTS,S has now received approval from Committee for Medicinal Products for Human Use (CHMP) of the European Medicines Agency (EMA) and World Health Organization will now develop a policy recommendation on the use of RTS,S/AS01, now commonly known as Mosquitrix™, in immunization programs. [34] Studies performed to assess cell-mediated immune responses indicated that although RTS,S induces both antibody responses against CS protein and $CD4^+$T cell responses, specific $CD8^+$ T cell responses were weak.[35]

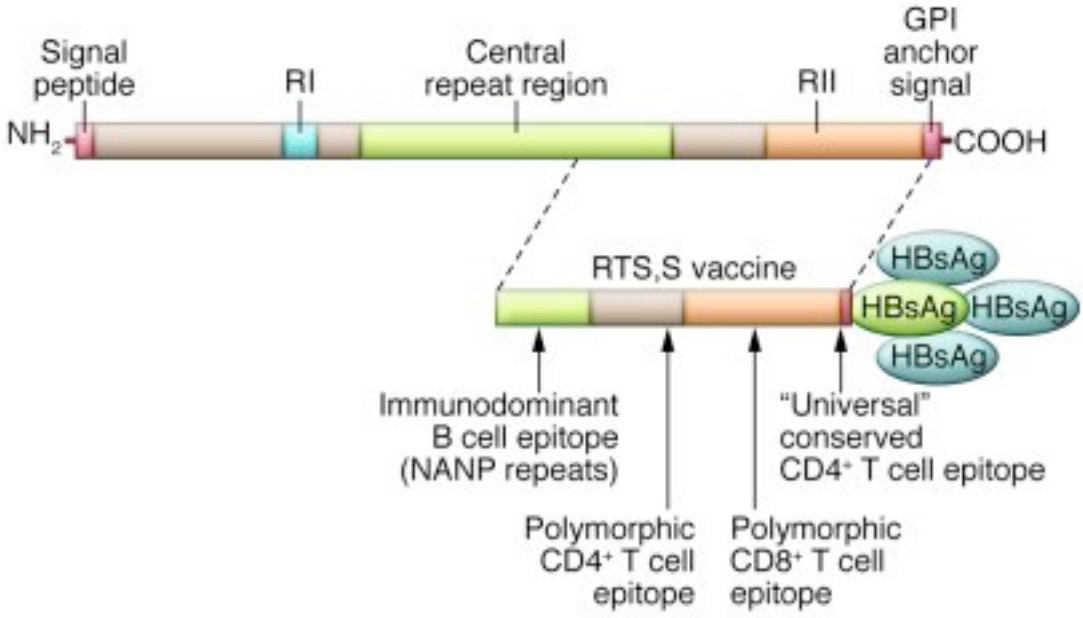

Figure 3: RTS,S particle composition.
HBsAg: Hepatitis B surface antigen;[36]

According to the 2013 WHO Malaria Vaccine Technology Roadmap a malaria vaccine should be available for used and licensed by 2030 have at least 75% efficacy. Therefore, the modest results from RTS,S/AS01 phase 3 clinical trials do not meet WHO guidelines and the search for a more effective vaccine continues. However, the effort and time required in clinical trials and the protection by vaccination in malaria-endemic areas are to be admired. [24] [25]

1.6.1.2 Whole-organism pre-erythrocytic malaria vaccines

Whole-organism pre-erythrocytic malaria vaccines rely on the use of the whole parasite, either attenuated or under antimalarial therapy, to elicit an immune response. [29]

Early work on malaria vaccines during the 1940s by Russell and Mohan with fowls immunized with *P. gallinaceum* and later by Freund *et al.* first with ducks immunized with *P. lophurae* and then with rhesus monkeys with *P. knowlesi* has shown that a whole-organism malaria vaccine can accomplish good protective efficacy against the parasite. [37] As previously mentioned, later work by Nussenzweig *et al.* showed that protective immunity could be induced in mice, and studies by Clyde *et al.* have shown that 90% of naïve human volunteers were immunized against *P. falciparum* after immunization with infected and irradiated mosquitoes. [37]

Whole-organism vaccines can be divided into 3 categories according to the method used to attenuate the parasite in order to elicit an immune response. The parasite can be attenuated, either by genetic manipulation or radiation, or it can be delivered live to volunteers taking antimalarial chemoprophylaxis.

a) Radiation-attenuated sporozoites (RAS)

Radiation-attenuated sporozoites prevail as the "gold standard" after studies in rodents and humans showed its sterilizing protection potential against *Plasmodium* infections.[27] [28] [38] RAS are incapable of division and differentiation. They are able to enter the hepatocytes but do not develop inside these cells. Nonetheless, they are able to trigger potent $CD8^+$ T cell responses, unlike heat-killed sporozoites that induce very low $CD8^+$ T cell responses. [39] [40] Studies have shown that these $CD8^+$ T cell responses are required for sterilizing immunity in malaria but it remains unclear how these cells are able to reduce the liver-stage parasite burden. [41] Immunizations with irradiated sporozoites have shown that two months after the immunization, the CS antigen continues to be presented. Importantly, this non-replicating antigen persists and is able to elicit immune responses by priming naïve T cells to acquire effector functions in order to clear the parasite in the liver long after immunization. [39]

RAS immunization has been the focus of the efforts by the US-based company, Sanaria™, who have developed PfSPZ, a malaria vaccine candidate that targets *P. falciparum* and consists of *P. falciparum* aseptic, purified and cryopreserved sporozoites attenuated by irradiation– metabolically active and non-replicative.[42] One downside of this vaccine is the route of administration. In animal models the common route is intravenous as it is the closest to the proboscis mosquito bite. However, an undetermined number of sporozoites are injected per mosquito and studies relying in mosquito bite are harder to standardize.[29] [43] Therefore, other routes of administration were evaluated and it has been shown that subcutaneous and intradermal sporozoite administration led to a suboptimal immunogenicity and protective efficacy.[44] For this reason, more recent clinical trials of this vaccine

candidate used either mosquito bites or intravenous injection as a method of immunization.[40] [45]

Although this strategy of malaria vaccination is able to elicit strong immune responses, it needs around 1000 irradiated *P. falciparum* infected mosquitoes to achieve that since the parasite it is not able to fully develop in the liver [42] whereas using CPS vaccination approach (see below) only 12-15 mosquitoes are required per immunization.[46] Moreover, this vaccination approach requires the availability of biosafety level III laboratories, since *P. falciparum* infected mosquitoes represent a risk of infection to humans. Another downside of this vaccination approach is that it only delivers antigens against one species of *Plasmodium*, not being able to meet the WHO Malaria Vaccine Technology Roadmap guidelines.

b) Genetically attenuated parasites (GAP)

Genetically attenuated malaria parasites were firstly developed in 2005 by deleting essential genes for liver-stage development of *Plasmodium* through the method of gene targeting that allows, by homologous recombination, the inactivation or modification of a gene. [47] [48] [49] [50] If this strategy is to be used as a method of sporozoite attenuation, the gene targeted for deletion has to be essential in liver-stage development in order for the parasite to be arrested in the liver and be unable to proceed with blood stage infection. However, this gene cannot be essential in blood stage, sexual and mosquito stage development, since blood stage parasites are required to the current transgenesis methods, and a normal development in the mosquito is needed for the production of sporozoites. It is also essential that the GAP lack drug-resistance markers, therefore meeting regulatory concerns in genetically attenuated organisms in vaccines.[30] It is also important that the GAP is created by double crossover recombination instead of single crossover recombination, making the parasite incapable of reverting to the wild-type phenotype and complete liver-stage development. [30]

One example of this vaccination strategy includes the deletion of UIS (upregulated in infective sporozoites) genes – essential to early liver-stage development. The UIS3 gene was successfully deleted in *P. berghei* and immunizations in rodents with this genetically attenuated parasite have proved to be capable of sterile immunity when challenged with wild type sporozoites and no breakthroughs were observed. However, this immunity is only active against pre-erythrocytic stages since parasitaemia was observed in mice when challenged with blood-stage parasites. [49] UIS4 gene has also been deleted in *P. berghei* and immunizations in mice have shown that this parasite is also capable of sterile immunity. However, when higher doses of sporozoites were administered intravenously (50,000 sporozoites vs 1,000 sporozoites) mice became infected with blood-stage parasites and genotyping confirmed that the blood-stage parasites were UIS4 knockout, therefore the parasite did not revert to wild-type. [48]

Another GAP vaccine candidate relies on the double knockout of *p52* and *p36* genes that are shown to be essential in establishing the parasitophorous vacuole, therefore the deletion of these genes results in early liver-stage

developmental arrest. [51] Initial studies carried out this double knockout parasite in a rodent model demonstrated that this model of a GAP vaccine is capable of inducing sterile protection and no breakthroughs were reported. [52] Later, a double knockout with human parasite *P. falciparum* orthologous genes was performed [52] and human trials were performed in order to test safety and immunogenicity of this vaccine candidate. [51] Volunteers were first exposed to 5 mosquito bites and then to 200 mosquito bites employing mosquitoes infected with the double knockout *P. falciparum* parasite developed immune responses against the repeat region of the CS protein, whereas volunteers exposed to only 5 mosquito bites did not. However, 12 days after the second mosquito bite, one volunteer presented blood stage parasites. After genotyping, it was shown that these parasites were indeed the double knockout parasite and therefore the parasite did not revert to the wild type. As recently shown in rodent model of malaria, *p52* and *p36* mutants are rarely capable of establishing an infection in a hepatocyte without the formation of a parasitophorous vacuole, which could explain the presence of blood stage parasites in one of the volunteers. Although this study showed promising results in terms of elicited antibody responses, investigation should proceed in optimizing multiple gene deletion responsible for essential steps in the liver stage development.[51]

Although this vaccination approach has the major advantage of a homogenous population of parasites where the genetic identity and phenotype can be defined in order to elicit optimal immune responses comparable with irradiated attenuated sporozoites immunizations, [30] as rodent studies and early human trials show, it is not risk-free since rare events may occur where the parasite is able to complete is life-cycle.

c) Chloroquine Chemoprophylaxis with Sporozoites (CPS)

Sterile immunity against *Plasmodium* was shown to be achieved by immunizing rodents with *P. berghei* while treating them with chloroquine, a drug known to kill asexual blood-stage parasites but not liver-stage parasites.[53]

Studies in humans have also shown that sterile immunity can be accomplished employing a drug-sensitive strain of *P. falciparum*, under chloroquine prophylaxis. Moreover, these studies have demonstrated to be more efficient in terms of protection that RAS immunizations since the latter requires a significantly higher number sporozoites to elicit sterile protection. [46] [54] Thirty-two months after the initial immunization, volunteers were re-challenged with infected *P. falciparum* mosquitoes and four out of six volunteers were negative for blood-stage parasites, while the other two had a delay in parasitemia.[55] It has been shown in studies using two groups of immunized individuals either by *P. falciparum* sporozoite inoculation under chloroquine treatment or with *P. falciparum* infected erythrocytes under chloroquine treatment that sterile protection is achieved by immune responses against the pre-erythrocytic stage only. The group inoculated with *P. falciparum* infected erythrocytes under chloroquine treatment skipped all the pre-erythrocytic stage of *Plasmodium* life-cycle and therefore was susceptible against a sporozoite challenge, whereas the group immunized with *P.*

falciparum sporozoites under chloroquine treatment were all protected against a sporozoite challenge. Nonetheless, none of the groups were protected against a challenge with *P. falciparum* infected erythrocytes nor was a difference in the period of parasitaemia appearance.[56]

Even though this immunization strategy is capable of eliciting sterile protection, it does not represent a possible strategy to be broadly implemented as it relies on the administration of fully infectious *P. falciparum* sporozoites. Nonetheless, it is a remarkable model to study immune responses against malaria.[46]

1.7 Rodent models of *Plasmodium* infection

1.7.1 *Plasmodium berghei* as a model to study malaria

Studying malaria in humans, although desirable, bears a lot of limitations. The ability to study the entire life-cycle is hindered by the lack of access to post-mortem organs and tissue samples. Even if access to these tissues is possible, they represent only the end stage of a complex life-cycle, and access to the events that led to this stage, such as the pre-erythrocytic stage or the study of cerebral malaria, is very limited. Moreover, it is not possible to control the immune responses in such studies. Therefore, the study of malaria has relied on the use of rodents for decades and such studies greatly contributed to a better understanding and knowledge of the parasite biology and host-parasite interactions. [57 58]

There are several species of *Plasmodium* known to infect rodents – *P. berghei, P. yoelii, P. chabaudi* and *P. vinckei* – and several of strains available in each species.[4 57] Regarding rodent-infectious *Plasmodium* parasites, *P. berghei* is widely used to study severe malaria clinical outcomes such as cerebral malaria, placental malaria, malaria-associated acute lung injury, acute kidney injury, severe malarial anemia and liver injury. [57] Although the scope of disease manifestations may vary between species and hosts, this must be seen has a reflection of the diversity in human disease and immunity.[57 58]

1.7.2 *Plasmodium berghei* as a vaccination approach

Several vaccine candidates began with studies in rodent models of malaria, and even though they were not able to anticipate the success in human trials, they reliably conclude which ones were not. [58]

Recently, the Prudêncio Lab at Instituto de Medicina Molecular has been working on a new whole-organism pre-erythrocytic malaria vaccine using a genetically modified *P. berghei* parasite as a method of presenting the immunogenic antigens of human infective *Plasmodium* spp. to the human immune system (see section 1.9.1). In order to accomplish the development of this new vaccine candidate, three premises had to be validated regarding *P. berghei* infectivity and immunogenicity: (1) Using *in vitro* human hepatoma

cell lines, *ex vivo* cultures of human primary hepatocytes and *in vivo* liver-humanized mouse models (^{LH}mice) it was demonstrated that *P. berghei* can infect and develop within human liver cells. Therefore, is able to present antigens that will generate the immune response required from a pre-erythrocytic vaccine; (2) *P. berghei* is not known to cause human pathology, thereby ensuring higher safety levels than previous whole organism vaccine approaches. Moreover, using blood-humanized mice (^{BH}mice), it was experimentally demonstrated for the first time that *P. berghei* parasites have very low infectivity of RBCs, and even though some merozoites are able to infect human erythrocytes, they are incapable of multiplying and therefore causing disease; (3) A genetically modified *P. berghei* expressing the selected antigen is able to elicit an immune response capable of protecting against a subsequent *P. falciparum* infection (Unpublished data).

1.8 Circumsporozoite Protein as the immunodominant antigen in *Plasmodium*

The circumsporozoite protein (CSP) is the most abundant protein in *Plasmodium* sporozoites. In the sporozoite surface, the CSP forms a dense coat and has been shown that plays a role in gliding motility. In the oocyst, CSP is essential for sporozoite formation and it is believed to be required to establish infection in the host's liver.[59] [60] The structure of CSP is highly conserved among *Plasmodium* species infecting rodents, primates and humans.[60] CSP is composed by a central repeat region, differing through *Plasmodium* species. This central repeat region is flanked by two highly conserved domains: Region I and region II. Region I is a 5-aminoacid sequence at the N-terminus and region II has a thrombospondin repeat at C-terminus. [60] *P. vivax* CSPs may differ around the world between VK210 and VK247. These two types of CSPs diverge in the central repeat region. [61]

Studies with transgenic mice expressing *P. yoelii* CS gene under constitutive promoter control have shown that the circulating CS is able to inhibit the infectivity of live sporozoites when injected intravenously or by mosquito bite. The results from these studies show that CSP is an immunodominant protective antigen in humoral responses against *Plasmodium* infections. [62]

Moreover, in a study where irradiated sporozoites immunized WT mice were compared with CSP-Tg/JhT(-/-) BALB/c irradiated sporozoites immunized mice, T-cell responses were evaluated by IFN- γ ELISPOT of mouse splenocytes. CSP-Tg/JhT(-/-) BALB/c mice are transgenic for the CS and unable to make antibodies. The authors reported that $CD8^+$ T-cell responses to non-CSP antigens were 20-100 times lower than those against CSP.[63]

As mentioned above, the most advanced malaria vaccine candidate until date, RTS,S is based on the CSP of *P. falciparum*.

1.9 Genetic transformation of *Plasmodium berghei*

In 2011, Lin, J. *et al.* developed the gene insertion/marker out (GIMO) method for transgene expression in rodent malaria parasites. This method allows the simultaneous introduction of heterologous proteins and removal of a drug-selectable marker. [64]

In this report, the authors designed and constructed a mother line ($GIMO_{PBANKA}$ for *P. berghei)* where a *hdhfr::yfcu* selectable marker is stably integrated into the non-essential *230p locus* present in chromosome 3. The gene of interest is integrated into the same locus by double cross-over homologous recombination, replacing the *hdhfr::yfcu* selectable marker cassette. These parasites can be negatively selected – as the motherline expressing the *yfcu* gene will not survive the 5-FC treatment. 5-FC is the drug 5-fluorocytosine that will kill all parasites expressing *yfcu.* [64]

1.9.1 *Plasmodium berghei* expressing *Plasmodium falciparum* CS

Previous studies performed in the Prudêncio Lab with a transgenic *P. berghei* expressing *P. falciparum* CS under the control of *P. berghei* UIS4 promoter (*Pb*(*Pf*CS@UIS4)), generated by the GIMO method (Figure 4), showed that this parasite has salivary gland and hepatic infectivities similar to wild-type *P. berghei* (Unpublished data), overcoming the limitations of a previously assayed transgenic parasite, where the endogenous CS was replaced by *P. falciparum* CS (*Pb*(*Pf*CS)), which was shown to have low mosquito salivary gland and hepatic infectivities. [65]

As previous stated, this transgenic *P. berghei* parasite is able to i) infect human hepatocytes *in vivo*; ii) unable to cause a human blood-stage infection that leads to pathology; iii) immunizations with *Pb*(*Pf*CS@UIS4) parasites elicits immune responses against a *P. falciparum* infection.

Further studies, using a non-natural host species, the New Zeeland White rabbit, as a model of *P. berghei* infection demonstrated that *P. berghei* is able to infect rabbit primary hepatocytes *ex vivo* and rabbit livers *in vivo*. However, blood-stage forms of the parasite were never detected in circulation in the rabbit. In order to assess infectivity of the merosomes developed in rabbit primary hepatocytes, merosomes were collected from the culture supernatant and injected into naïve mice. After around 7 days post-infection, mice were positive for blood-stage parasites (Unpublished data).

Humoral responses were analyzed in both mice and rabbits after immunizations with *Pb*(*Pf*CS@UIS4) and results show high titers of anti-*Pf*CS antibodies in the serum of these animals. Moreover, serum from mice immunized with *Pb*(*Pf*CS@UIS4) is able to recognize and bind with high avidity to *P. falciparum* sporozoites and is capable to functionally inhibit *P. falciparum* hepatic invasion (Unpublished data).

Cellular responses were analyzed by ELISPOT assay with splenocytes of *Pb*(*Pf*CS@UIS4) immunized mice and results showed that *P. berghei*/

Pb(*Pf*CS@UIS4) elicit cross-species cellular immune responses against *P. falciparum,* which are not dependent on the presence of the *Pf*CS immunogen on the *P. berghei* parasite.

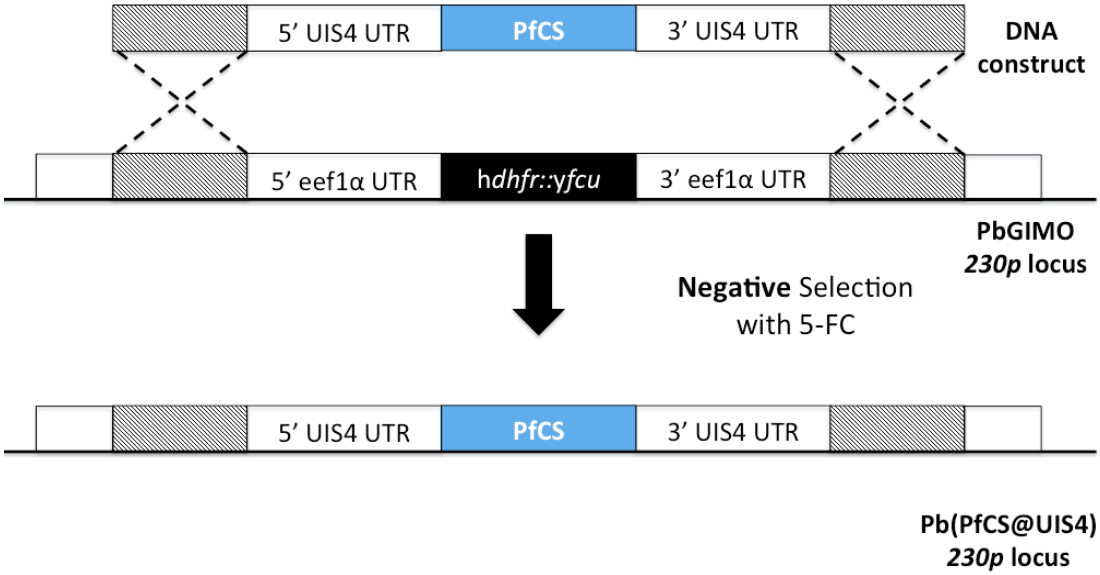

Figure 4: Schematic representation of Pb(PfCS@UIS4) through the GIMO transfection method.

1.9.2 *Plasmodium berghei* expressing *Plasmodium vivax* CS

In 2013, a transgenic *P. berghei* expressing *P. vivax* CS under the control of the *P. berghei* UIS4 promoter (*Pb*(*Pv*CS@UIS4)) was generated by Inês Albuquerque, employing the GIMO method. This parasite was further characterized by Miguel Duarte and, similarly to *Pb*(*Pf*CS@UIS4), *Pb*(*Pv*CS@UIS4) was shown to have normal sporogonic development and hepatic infectivity similarly with the wild-type *P. berghei* (Unpublished data). Even though this characterization showed positive results, no immunization studies were yet performed with this parasite.

1.9.3 *P. berghei* simultaneously expressing *P. falciparum* and *P. vivax* CS

Due to the success of *Pb*(*Pf*CS@UIS4) and preliminary studies with *Pb*(*Pv*CS@UIS4) having shown to being identical in terms of sporogonic, *in vitro* and *in vivo* development to the wild-type , and in compliance with the World Health Organization guidelines, the Prudêncio Lab decided to generate a *P. berghei* transgenic parasite simultaneously expressing CS of *P. falciparum* and *P. vivax* in non-essential *loci* under the control of *P. berghei* UIS4 promoter – *Pb*TriCS.

Therefore, at the Leiden University Medical Center, the *hdhfr::yfcu* selectable marker was stably integrated into the non-essential *S1 locus* present in

chromosome 12 of the Pb(PfCS@UIS4) transgenic parasite. The *S1 locus* has been previously characterized as a dispensable *Plasmodium* locus in *P. berghei* and *P. yoelii*. [66] After the integration of the selectable marker in *Pb*(*Pf*CS@UIS4) *S1 locus*, Joana Pissarra generated the *Pb*TriCS parasite by stably integrating the gene encoding *P. vivax* CS into that locus by double cross-over homologous recombination, using the GIMO method to replace the *hdhfr::yfcu* selectable marker cassette (Figure 5).

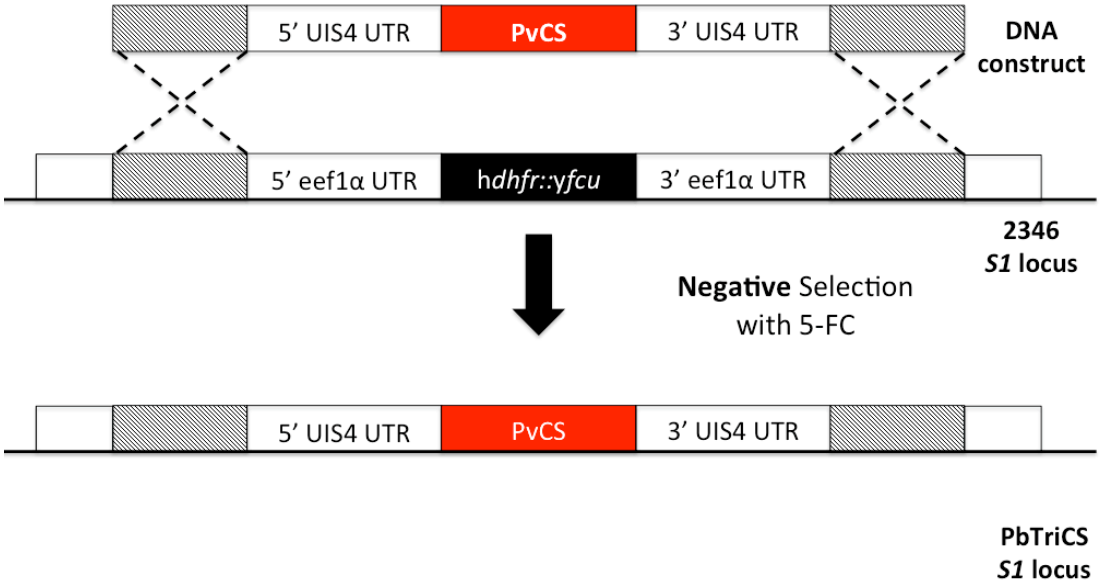

Figure 5: Schematic representation of PbTriCS transfection through the GIMO transfection method.

Hence, the newly generated *P. berghei* parasite simultaneously expresses three CS proteins: the *P. berghei* endogenous CS, expressed in the native locus (chromosome 4), the *P. falciparum* CS expressed in the *230p locus* (chromosome 3), and the *P. vivax* CS expressed in the *S1 locus* (chromosome 12).

AIMS

2

2. Aims

During this project we used a *P. berghei* parasite expressing both *P. falciparum* and *P. vivax* CS proteins. It is important that its development is not impaired by the double gene knock-in nor by the expression of multiple CS proteins. We envisage that immunizations using this parasite will lead to protection against both *Plasmodium* species.
To address these questions we propose:

- To genotype *Pb*TriCS in order to evaluate correct integration of the gene of interest (GOI) and removal of the selectable marker in the *S1* locus.
- To assess the development of *Pb*TriCS in *Anopheles* mosquitoes, in terms of oocysts production and sporozoite infectivity of salivary glands.
- To characterize *Pb*TriCS liver cell infectivity and development *in vitro* using a human hepatoma cell line as a model.
- To characterize *Pb*TriCS liver infectivity and development *in vivo* using C57BL/6J mice as a model.
- To assess CS expression and localization in sporozoites as well as in EEFs *in vitro* and *in vivo.*
- To assess humoral responses against CS peptides elicited by *Pb*TriCS-immunization of mice.

MATERIALS & METHODS

3

3. Materials & Methods

3.1 Parasite Lines

$GIMO_{PbANKA}$
Plasmodium berghei GIMO (Gene insertion/ marker out) [64] is a clonal parasite line provided by the Shahid Khan & Chris Janse Lab in the Leiden University Medical Center (Netherlands) and is used during this project as a control (wild-type) since it was used as the transfection motherline for the generation of *Pb*(*Pf*CS@UIS4) and *Pb*(*Pv*CS@UIS4). $GIMO_{PbANKA}$ has a positive/negative selection marker cassette (*hdhfr*::*yfcu*) at the 230*p* locus.

Pb(*Pf*CS@UIS4)
*Plasmodium berghei Pf*CS@UIS4 is a clonal parasite line expressing *Plasmodium falciparum* CS protein under the control of *Plasmodium berghei* UIS4 promoter at the 230*p* locus. This parasite was produced by the Shahid Khan & Chris Janse Lab in the Leiden University Medical Center (Netherlands) through the GIMO transfection method. [64]

2346
Plasmodium berghei 2346 is a clonal parasite line used as a transfection motherline of *Pb*TriCS and was provided by Leiden Medical University Center. This parasite expresses *Plasmodium falciparum* CS protein under the control of *Plasmodium berghei* UIS4 promoter at the 230*p* locus and has a positive/negative selection marker cassette (*hdhfr::yfcu*) at the *S1* locus.

*Pb*TriCS
Plasmodium berghei Triple CS is a clonal parasite line that expresses the endogenous *P. berghei* CS protein, *Plasmodium falciparum* CS protein under *Plasmodium berghei* UIS4 promoter at 230*p* locus and *Plasmodium vivax* CS protein under *Plasmodium berghei* UIS4 promoter at *S1* locus. Joana Pissarra produced this transgenic parasite through the GIMO transfection method.[64] Two independent transfections were performed and two clones were selected for further characterization (*Pb*TriCScl1 and *Pb*TriCScl2).

3.2 Genotyping

Correct integration of the *Pv*CS@UIS4 cassette into the *S1* genomic locus of 2346 was confirmed by 4 different PCR reactions:

- 5' integration region;
- 3' integration region;
- selectable marker (*hdhfr::yfcu*);
- gene of interest (*Pv*CS@UIS4).

PCR reactions are detailed bellow (Table 1, 2 and 3), such as the primers sequences used for the amplification of each region (Table 4).

Table 1: PCR reaction components mixture

PCR reaction components	Volume per reaction
10 x buffer	5 µL
50 mM $MgCl_2$	3 µL
10mM dNTPs	1,25 µL
Genomic DNA	50ng
Primer Foward (10 µM)	2,5 µL
Primer Reverse (10 µM)	2,5 µL
NZYTech DNA Taq Polymerase	0,4 µL
H_2O	Up to 50uL of final volume

Table 2: PCR reaction program for 5' integration, 3' integration and selectable marker

95°C	2m
95°C	30s
57°C	10s
59°C	10s
61°C	10s
72°C	90s
72°C	2m

x 30 cycles

Table 3: PCR reaction program for gene of interest (*Pv*CS@UIS4)

95°C	2m
95°C	30s
60°C	10s
62°C	10s
72°C	65s
72°C	2m

x 30 cycles

Table 4: Primers used and correspondent sequences and amplicons

Region	Primers	Sequence	Amplicon
5' Integration	F: 1820	5'GCATGTGCATGTATACTATCTAAC3'	1036bp
	R: 1821	5'AGAAGCATTCCTTATTGTTCAG3'	
3' Integration	F: 1824	5'GAAGCAGCCGTATATGCAAAC3'	1348 bp
	R: 1825	5'ACGGACAATACAGATAGTAAACAG3'	
Selectable Marker	F: 1901	5'GTTCGCTAAACTGCATCGTC3'	1100 bp
	R: 1902	5'GTTTGAGGTAGCAAGTAGACG3'	
Gene of Interest	F: 1822	5'GCTGTTTCTTCCATCCTGTTG3'	1083 bp
	R: 1823	5'GACTAGCCCTAATGAATTACTCAC3'	

PCR reactions were analyzed by gel electrophoresis on a 1% agarose gel stained with RedSafe™ Nucleic Acid Staining Solution and revealed on Chemidoc XRS+.

3.3 Sporogonic Stage

3.3.1 Mosquitoes and *Plasmodium berghei* life cycle maintenance

Anopheles stephensi mosquitoes were produced in IMM's Insectary Facility at 28°C and 80% humidity under a 12 hours light/dark cycle.
Infection of the mosquitoes with the specific parasite lines was performed by Ana Filipa Teixeira by allowing the mosquitoes to blood-feed on infected mice at around 3% parasitaemia, after confirmation of male gametocyte exflagellation. Following the blood meal, mosquitoes were kept at 20°C and 80% humidity under a 12 hours light/dark cycle.

3.3.2 Oocysts

Between 12 and 13 days after the infective blood meal, mosquitoes were hand-dissected in 1x PBS and midguts were collected in order to count oocysts.
Midguts were later stained by immersion on 2% Mercurochrome solution to intensify contrast and mounted on a glass slide. Oocysts in the mosquito midgut wall were observed and counted on an Olympus CX41 optical microscope at 200x or 400x amplification.

3.3.3 Sporozoites

At 16, 18, 21 and 24 days post-infection, different mosquito tissues were hand dissected in order to count sporozoites developing inside oocysts lodged on the midgut wall, free in the hemolymph, and inside the mosquito's salivary glands.
Tweezers were used to expose the mosquito midgut and a cut was performed in the mosquito proboscis to collect hemolymph with a micropipette. Mosquito salivary glands were obtained by hand-dissection in RPMI medium using needles.
After dissection, tissues and sporozoites were always kept on ice. Mosquito's midguts and salivary glands were homogenized by compression with pestle against the wall of a microcentrifuge tube, followed by filtration trough a 70 μM strainer. After homogenization, sporozoites were on a Neubauer chamber using an Olympus CKX41 inverted microscope. Since no homogenization is necessary for sporozoites free in the mosquito's hemolymph, sporozoites were directly counted on a Neubauer chamber using an Olympus CKX41 inverted microscope.

3.4. *In vitro* Characterization of *Pb*TriCS

Huh7 is a human hepatoma cell line that was established from a hepatocellular carcinoma. [67]

Twenty-four hours prior to infection, Huh7 hepatoma cells in RPMI complete medium (supplemented with 10% Fetal Bovine Serum [FBS], 1% Penicillin-Streptomycin, 1% Glutamine, 1% Non-essential Amino Acids and 1% HEPES [4-(2-hydroxyethyl)-1-piperazineethanesulfonic acid]) were seeded in a 24 well-plate with a glass coverslip, at the confluence of $5x10^4$ cells per well. Cells were kept at 37°C and 5% CO_2.

At 0 hours, cells were infected with $3x10^4$ sporozoites per well with RPMI complete medium supplemented with 1:300 dilution of fungizone to prevent contamination by fungi. After infection, the 24 well-plate was centrifuged at 3000 rpm during 5 minutes and at 2 hours post-infection medium was changed to fresh medium. At 24 and 48 hours post infection, cells were fixed with 4% paraformaldehyde for 10 min and stored at 4°C.

3.4.1 Immunofluorescence microscopy

Proceeding fixation, coverslips with infected Huh7 cells were simultaneously blocked and permeabilized with a solution of 1% Bovine Serum Albumin (BSA) and 0,2% Triton X-100 in 1x PBS. The following primary antibodies were then employed at different concentrations:

- α-UIS4 (binding *P. berghei* UIS4 protein)
- 3D11 (binding *P. berghei* CS protein),
- 2A10 (binding *P. falciparum* CS protein)
- 2F2 (binding *P. vivax* CS protein).

The latter 3 antibodies were isolated from mouse hybridomas meaning that each coverslip could only have one of them combined with α-UIS4 (goat). Secondary antibodies incubation followed primary antibodies incubation after 3 washes with 1x PBS, have being used Alexa-Fluor 488 (anti-mouse, Donkey IgG), Alexa-Fluor 567 (anti-goat, Donkey IgG) and Hoechst (for DNA staining – nuclei). Coverslips were mounted using Fluoromount G (Southern Biotech).

Images were acquired using a Zeiss Axiovert 200M Widefield Fluorescence Microscope at 200x magnification.

3.4.1.1 EEF Size and relative number quantification

Images were acquired using a Zeiss Axiovert 200M Widefield Fluorescence Microscope at 200x magnification and were analyzed using ImageJ 1.47v software. For each coverslip, the number of EEFs was counted as well as the number of nuclei. Subsequently, the number of EEFs was normalized to the number of nuclei per coverslip in order to quantify infectivity. Images representing the CS protein expression and localization were taken using Zeiss LSM 510 META confocal point-scanning microscope with a 63% oil objective.

3.4.2 Gliding Motility Assay

Coverslips were coated with anti-CS monoclonal antibodies (3D11, 2A10 and 2F2) and $3x10^4$ sporozoites were added per coverslip followed by centrifugation at 3000 rpm during 5 minutes. After 1 hour incubation at 37°C and 5% CO_2, sporozoites were fixed using 4% paraformaldehyde and then blocked using 1% BSA in PBS. Later, coverslips were stained using the same primary antibody and Alexa-Fluor 488 (anti-mouse, Goat IgG) as a secondary antibody, after 3 washes with 1xPBS. Coverslips were then mounted using Fluoromount G and analysis was performed using Leica DM5000B widefield fluorescence microscope with a 40% objective.

3.4.3 Cell Traversal Assay

Twenty-four hours prior to infection, Huh7 cells were seeded in the conditions described above in a 24-well plate with $5x10^4$ cells per well. At 0 hours, $3x10^4$ sporozoites were added per well in RPMI complete medium with 0,5 mg/mL fluorescein isothiocyanate (FITC) dextran and the plate was centrifuged for 5 minutes at 3000 rpm. After 2 hours post-infection, the cells were trypsinized and RPMI complete medium was added after 5 minutes and cells were centrifuged at 1200rpm for 5 minutes. Cells were then ressuspended in 2% Fetal Bovine Serum (FBS) and kept on ice. Analysis of the parasite traversal ability was performed using BD Biosciences LSR Fortessa cell analyzer.

3.5 *In vivo* Characterization of PbTriCS

3.5.1 Mice

In vivo experiments were performed using C57BL/6J from Charles River Laboratories International. Mice were housed in specific-pathogen-free rodent facility at Instituto de Medicina Molecular. All *in vivo* experiments were performed in agreement with national and European regulations and were approved by internal animal care committee of the Instituto de Medicina Molecular.

3.5.2 Liver Infection

C57BL/6J Mice were infected with sporozoites obtained by the dissection of *A. stephensi* mosquitoes as stated above and were injected intravenously with $3x10^4$ sporozoites. At 6 hours or at 46 hours post infection, mice were sacrificed and livers were collected to quantify parasite liver load. Defined lobes were fixed with 4% paraformaldehyde and later used for immunofluorescence microscopy. The remaining lobes were flash-frozen in liquid nitrogen and used for qRT-PCR analysis.

For the clodronate experiment, 48 hours before infection, mice were injected intravenously with PBS liposomes (control group) or clodronate liposomes (to cause apoptosis of macrophages). At 0 hours, mice were infected with $3x10^4$ sporozoites per mouse and everything followed as a normal infection.

3.5.2.1 RNA isolation, cDNA synthesis and qRT-PCR quantification

For mouse liver RNA extraction, livers were homogenized in Denaturing Solution (4 M guanidine thiocyanate, 25 mM sodium citrate [pH 7], 0.5% *N*-lauroylsarcosine in diethyl pyrocarbonate [DEPC]-treated water) supplemented with 0,1 M β-mercaptoethanol and RNA was extracted using Quiagen's RNeasy Mini Kit according to manufacturer's instructions. Total RNA was quantified using NanoDrop 1000 spectrophotometer and cDNA was synthetized using the NZYTech First-Strand cDNA synthesis kit. The cDNA reaction mixture and thermo cycler reaction program are detailed bellow in tables 5 and 6, respectively.

Table 5: cDNA reaction mixture

cDNA reaction components	Volume per reaction
10x Buffer	2 µL
50 µg/mL Random Hexamer	1 µL
400 U/µL Rnase Inhibitor	0,5 µL
10 mM dNTPs mix	1 µL
200 U/µL Reverse Transcriptase	1 µL
Template RNA	5 µg
H2O	Up to 20µL of final volume

Table 6: cDNA thermo-cycler reaction program

25°C	10 minutes
55°C	30 minutes
85°C	5 minutes

Following cDNA synthesis, gene expression analysis was performed using Bio Rad Kit.

For analysis of parasite load in the liver, *P. berghei* 18S mRNA gene expression level was normalized against the Hypoxanthine-guanine phosphoribosyltransferase (HPRT) housekeeping gene using the comparative threshold cycle (C_T). The ratio between 18S and HPRT was calculated as follows: $2^{HPRT}/2^{18S}$.

For the clodronate experiment, to evaluate the successful action of clodronate liposomes, qRT-PCR was performed targeting 3 different genes: Clec4F

(Kupffer cells), CD68 (monocytes/macrophages) and F4/80 (differentiated macrophages). Analysis was performed as stated above. Gene expression was normalized against HPRT, a mouse housekeeping gene and the ratio was calculated as $2^{HPRT}/2^{target\ gene}$. qRT-PCR components mixture, reaction program and primers used are detailed in tables 7, 8 and 9, respectively.

Table 7: qRT-PCR components mixture

qRT-PCR components	Volume per reaction
SYBRGreen Master Mix	10 µL
Primer Forward	0,4 µL
Primer Reverse	0,4 µL
H_2O	7,2 µL
cDNA template	2 µL

Table 8: qRT-PCR reaction program

50°C	2 minutes	
95°C	10 minutes	x 40 cycles
95°C	15 seconds	
60°C	1 minute	
95°C	15 seconds	
60°C	1 minute	
95°C	30 seconds	
60°C	15 seconds	

Table 9: Primers used in qRT-PCR analysis

Gene	Primers	Sequence
18S rRNA	F: 33	5'AAGCATTAAATAAAGCGAATACATCCTTAC3'
	R: 34	5'GGAGATTGGTTTTGACGTTTATGTG3'
HPRT	F: 249	5'TTTGCTGACCTGCTGGATTAC3'
	R: 250	5'CAAGACATTCTTTCCAGTTAAAGTTG3'
Clec4F	F: 1096	5'TGAGTGGAATAAAGAGCCTCCC3'
	R: 1097	5'TCATAGTCCCTAAGCCTCTGGA3'
CD68	F: 1070	5'AGCTGCCTGACAAGGGACACT3'
	R: 1071	5'AGGAGGACCAGGCCAATGAT3'
F4/80	F: 1098	5'CCCCAGTGTCCTTACAGAGTG3'
	R: 1099	5'GTGCCCAGAGTGGATGTCT3'

3.5.2.2. Immunofluorescence microscopy

Following the fixation of the liver lobes with 4% paraformaldehyde, livers were sliced into 50 µm sections using a Leica VT1000S vibrotome.

Liver slices were then permeabilized and blocked with 0,5% Triton X 100, 1% BSA and IgG anti-mouse in PBS. After permeabilization, liver slices were

incubated with primary antibodies, using the following combinations: α-UIS4 + 3D11 (against *P. berghei* CS protein); α-UIS4 + 2A10 (against *P. falciparum* CS protein) and α-UIS4 + 2F2 (against *P. vivax* CS protein).

Secondary antibodies incubation followed primary antibodies incubation, have being used Alexa-Fluor 488 (anti-mouse, Donkey IgG), Alexa-Fluor 567 (anti-goat, Donkey IgG) and Hoechst (for DNA staining – nuclei). Liver slices were mounted on a microscope slide using Fluoromount G (Southern Biotech).

In order to count the number of EEFs per liver area and to measure the areas of those EEFs, liver slices were analyzed and images were acquired using Leica DM5000B widefield fluorescence microscope with a 20% objective. Images were analyzed using the ImageJ 1.47v software.

3.6 Assessment of humoral responses

3.6.1 Immunizations

In order to evaluate the humoral responses elicited by *Pb*TriCS, mice were immunized by intravenously injection of $5x10^4$ sporozoites at day 0. On the 3rd day after the first immunization, chloroquine was administered by intraperitoneal injection (1,4 mg/ mouse) and thereafter (0,7 mg/ mouse). On the 9th day after the first immunization, $3x10^4$ sporozoites were injected intravenously making the second immunization and tail blood was collected prior to sporozoite injection. Chloroquine administration resumed on the 12th (1,4 mg/ mouse) and thereafter (0,7 mg/ mouse). The third immunization took place on the 21st day after the first and tail blood was collected prior to sporozoite injection. Chloroquine treatment was resumed on the 24th day (1,4 mg/ mouse) and thereafter (0,7 mg/ mouse) until the 30th day. On the 33rd day tail blood was collected. After blood collection, blood was centrifuged at 3000 rpm for 5min to separate the red blood cells from the plasma. Plasma was then stored at -20°C until ELISA analysis.

3.6.2 ELISA

ELISA (enzyme-linked immunosorbent assay) measures the levels of antibodies in the sera of mice after immunization. 96-well ELISA plates were coated with CS repeats (Pb, Pf or Pv) diluted in Coating Buffer (0.1 M sodium carbonate, pH 9.5, 7.13 g NaHCO3, 1.59 g Na2CO3; q.s. to1.0 L; pH to 9.5 with 10 N NaOH) at a concentration of 2µg/mL and incubated overnight at 4°C.The next day, plates were washed 3 times with Elisa Wash (PBS 1x; 0,1% Tween 2.0) and then blocked with Elisa Buffer (PBS 1x; 1% BSA; 0,1% Tween 2.0) for half hour. After this time, plates were washed once and the wells were then filled with dilutions of the mouse serum from the three immunizations diluted in Elisa Buffer. The titration curve was designed with primary antibodies (α-PbCS 3D11;α-PfCS 2A10;α-PvCS 2F2) starting with a concentration of 0,05µg/µL and then diluted at 1:10. After incubation, plates were washed 3 times with Elisa Wash and next a solution of an animal antibody against mouse antibody was used. This second antibody, goat α-

mouse IgG, is covalently conjugated to the HRP (Horseradish Peroxidase) enzyme. Lastly, a solution of a colorgenic enzyme substrate (Hydrogen Peroxide) was added. The interaction of the Hydrogen Peroxide with the HRP conjugated to the second antibody generated visible color. The levels of antibodies in the serum increase along with color intensity and vice-versa. Color intensity was measured by Infinite® 200 PRO-Tecan spectrophotometer for a precise determination of the antibodies level present in the mice sera.

3.7 Statistical Analysis

Data is expressed as means ± standard error of the mean (SEM). Statistically significant differences between two different groups were analyzed using the Mann-Whitney non-parametric test with a 95% confidence interval. Results were considered not to be significantly different for a P value of >0.05 (ns). Under this value, all results were considered statistically significant. Levels of significance followed this convention: *, $P \leq 0.05$; **, $P \leq 0.01$; ***, $P \leq 0.001$; ****, $P \leq 0.0001$. All statistic tests were performed using Graph Pad Prism 6 software.

RESULTS

4

4. Results

4.1 Genotyping of the *Pb*TriCS parasite

Following a successful transfection, parasites are injected into mice to which the drug 5-FC is subsequently administered. This leads to the negative selection of parasites containing the *hdhfr::yfcu* gene (selectable marker- SM). Nonetheless, a small population of parasites usually escapes the negative pressure, meaning that that treatment with 5-FC does not generate a pure cloned line, but instead there is a mixed population of 2346 and *Pb*TriCS. For this reason, it is essential to perform a parasite dilution cloning after negative selection to obtain a pure clonal parasite population free of drug-selectable markers.

Parasite dilution cloning is a technique that consists of limiting dilutions of parasites in order to obtain only 0.5-2 parasites per 0.2ml of 1x PBS that is injected i.v. into mice. The aim is to inject a single parasite per mouse, either the non-transfected 2346 parasite or the successfully transfected *Pb*TriCS parasite, generating a pure clonal line from a single parasite. [68] Joana Pissarra performed two independent transfections followed by two independent cloning events, generating a total of four clones, two of which were selected for further characterization – *Pb*TriCScl1 and *Pb*TriCScl2. These two clones arose from independent transfections and were genotyped to confirm correct 5' and 3' integration and replacement of the *hdhfr::yfcu* gene by the *Pv*CS@UIS4 cassette (gene of interest – GOI) at *S1* locus as intended. (Figures 6A and 6B).

In order to warrant the correct 5' and 3' integration, primers were design to amplify DNA only in case of exact integration. As shown in Figure 6A, the 1820 forward primer binds upstream of the 5' targeting region and the 1821 reverse primer binds inside 5' *Pb*UIS4 UTR with an amplicon size of 1348 bp, while the 1824 forward primer binds inside the 3' *Pb*UIS4 UTR and the 1825 reverse primer binds downstream the 3' targeting region with an amplicon size of 1348 bp. To confirm a pure clonal line, a PCR reaction was performed with primers1901 (hdhfr forward) and 1902 (yfcu reverse) and no amplification is expected for *Pb*TriCS parasites; only in 2346 motherline is expect an amplicon with 1100 bp. Last, to ensure proper replacement of the SM by the GOI, the PvCS@UIS4 cassette, the 1822 forward primer and the 1823 reverse primer bind inside the *Pv*CS gene and an amplicon of 1083 bp is expected (Figure 6B).

Our results show that in both *Pb*TriCScl1 and *Pb*TriCScl2 the gene of interest successfully replaced the selectable marker and integrating correctly at the 5' and 3' end, since the band expected for the SM is only present in 2346 parasite. This indicates that both *Pb*TriCScl1 and *Pb*TriCScl2 are pure clonal lines with no non-transfected parasites being present in these populations (Figure 6C).

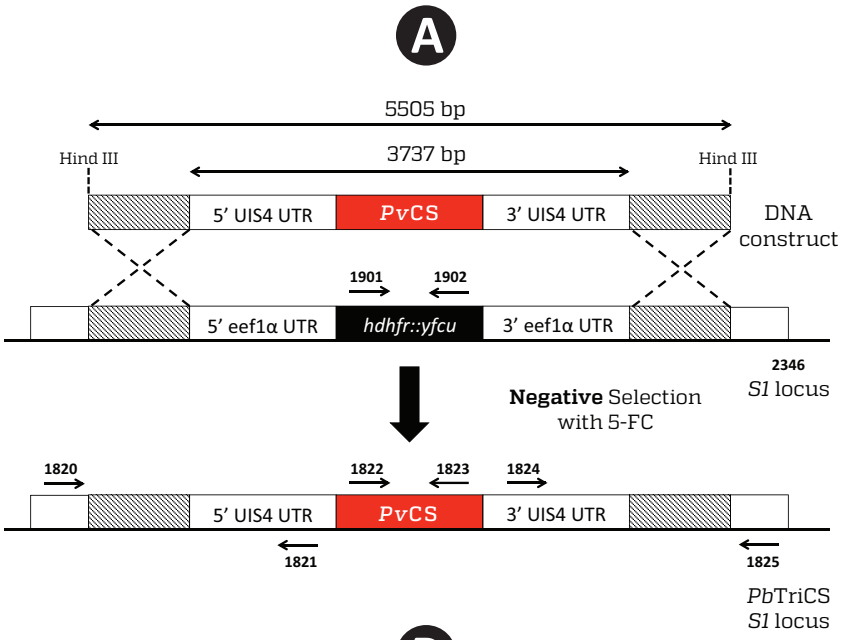

B

Background	Region	Primers		Amplicon
2346 (*Pf*CS@230p & hdhfr::yfcu@S1)	5'int S1	1820	F upstream 5' TR	No amplicon
		1821	R inside *Pb*UIS4 5'	
	3' int S1	1824	F inside 3' *Pb*UIS4 UTR	No amplicon
		1825	R downstream 3' TR	
	SM (hdhfr)	1901	F inside hdhfr	1100 bp
		1902	R inside yfcu	
	GOI (PvCS)	1822	F inside *Pv*CS	No amplicon
		1823	R inside *Pv*CS	
PbTriCS (*Pf*CS@230p & *Pv*CS@S1)	5'int S1	1820	F upstream 5' TR	1036 bp
		1821	R inside *Pb*UIS4 5'	
	3' int S1	1824	F inside 3' *Pb*UIS4 UTR	1348 bp
		1825	R downstream 3' TR	
	SM (hdhfr)	1901	F inside hdhfr	No amplicon
		1902	R inside yfcu	
	GOI (*Pv*CS)	1822	F inside *Pv*CS	1083 bp
		1823	R inside *Pv*CS	

C

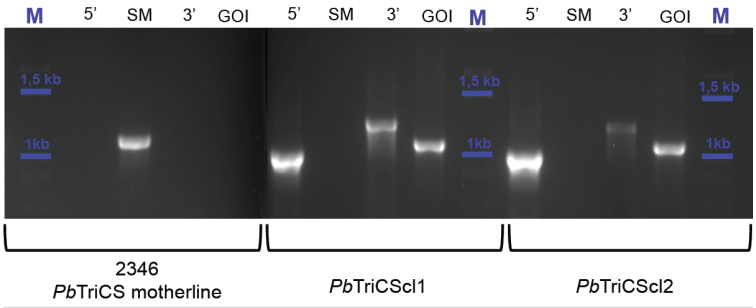

Figure 6: Genotyping of *Pb*TriCS parasites
A- *Pv*CS@UIS4 cassette integrated into 2346 motherline S1 locus through the GIMO transfection method. **B-** Table of primers used when genotyping *Pb*TriCS clones and respective amplicon size. **C-** Agarose gel analysis of PCR results. As demonstrated the SM present in the 2346 motherline is successfully replaced by the PvCS@UIS4 cassette.

4.2 Sporogonic Development of *Pb*TriCS

Upon genotyping of *Pb*TriCS parasites, the development of these parasite lines in *Anopheles* mosquitoes was assessed by comparison with wild-type *Pb*GIMO parasites.

4.2.1 *Pb*TriCS oocysts development in mosquito's midguts

The first step to evaluate the development and infection of *Pb*TriCS parasites inside the mosquito was to evaluate the impact of transfection in the capacity of the parasite to infect mosquitoes, generating oocysts. This was achieved by counting the number of oocysts present in the midgut basal lamina at 12-13 days post-infection. For *P*bGIMO, 5 experiments were performed where a total of 52 midguts were analyzed from which 96,2% were infected presenting an average of 211,1 ± 26,3 oocysts. For *Pb*TriCScl1, 5 experiments were carried out being analyzed a total of 49 midguts, where 95,8% was infected; 255 ± 23,8 oocysts. For *Pb*TriCS cl2, the clone available after the second transfection, 2 experiments were performed, where 25 midguts were analyzed of which 96% were infected; 220,7 ± 27,8 oocysts. Results are present in Figure 7A and are expressed as mean number of oocysts ± standard error of the mean. Our results show that *Pb*TriCS parasites are able to invade and develop within mosquito's midguts at the same level as *Pb*GIMO since the differences observed between parasites are not statistically significant.

4.2.2 Infectivity of *Pb*TriCS sporozoites towards mosquito salivary glands

In order to evaluate the ability of the sporozoites to develop inside the mosquito and reach the salivary glands, 10 mosquitoes per experiment were dissected at day 21 post-infection and the number of sporozoites present in the salivary glands was quantified. For *Pb*GIMO and *Pb*TriCScl1, 4 experiments were performed presenting a mean of 35586 ±7321 and 45738 ± 6273 sporozoites per mosquito, respectively. Results are presented in Figure 7B and are expressed as mean number of sporozoites per mosquito ± standard error of the mean. Our results show that *Pb*TriCS sporozoites are able to reach and invade the mosquito's salivary glands at the same level as *Pb*GIMO since the differences observed between parasites are not statistically significant.

Additionally, for one of the clones, *Pb*TriCScl1, sporozoite development was further characterized by performing 3 independent experiments to assess the number of sporozoites developing within oocysts in the mosquito's midguts as well as free in the mosquito's hemolymph and in the mosquito's salivary glands, over the course of 4 time points (days 16, 18, 21 and 24 post-infection) (Figure 7C).

The results are in agreement with sporogonic development of *Plasmodium* life-cycle as the number of sporozoites gradually increases in the mosquito's midguts until day 21, when it starts to decrease. Similarly, the number of sporozoites free in the mosquito hemolymph increases, accompanying the

expected release of sporozoites from the oocysts, and starts to decrease as sporozoites invade the salivary glands. In the salivary glands, the number of sporozoites increases gradually until the 24th day (last day observed). For each experiment, 10 mosquitoes were dissected per parasite in all time points. Results are presented in Table 10 and are expressed as mean number of sporozoites per mosquito ± standard error of the mean.

Our results suggest that the presence of two exogenous proteins in the *Pb*TriCS parasite does not prevent or significantly alter the conversion of parasites from oocysts to sporozoites in the mosquito midgut as well as their migration through the hemolymph and invasion of the mosquito salivary glands.

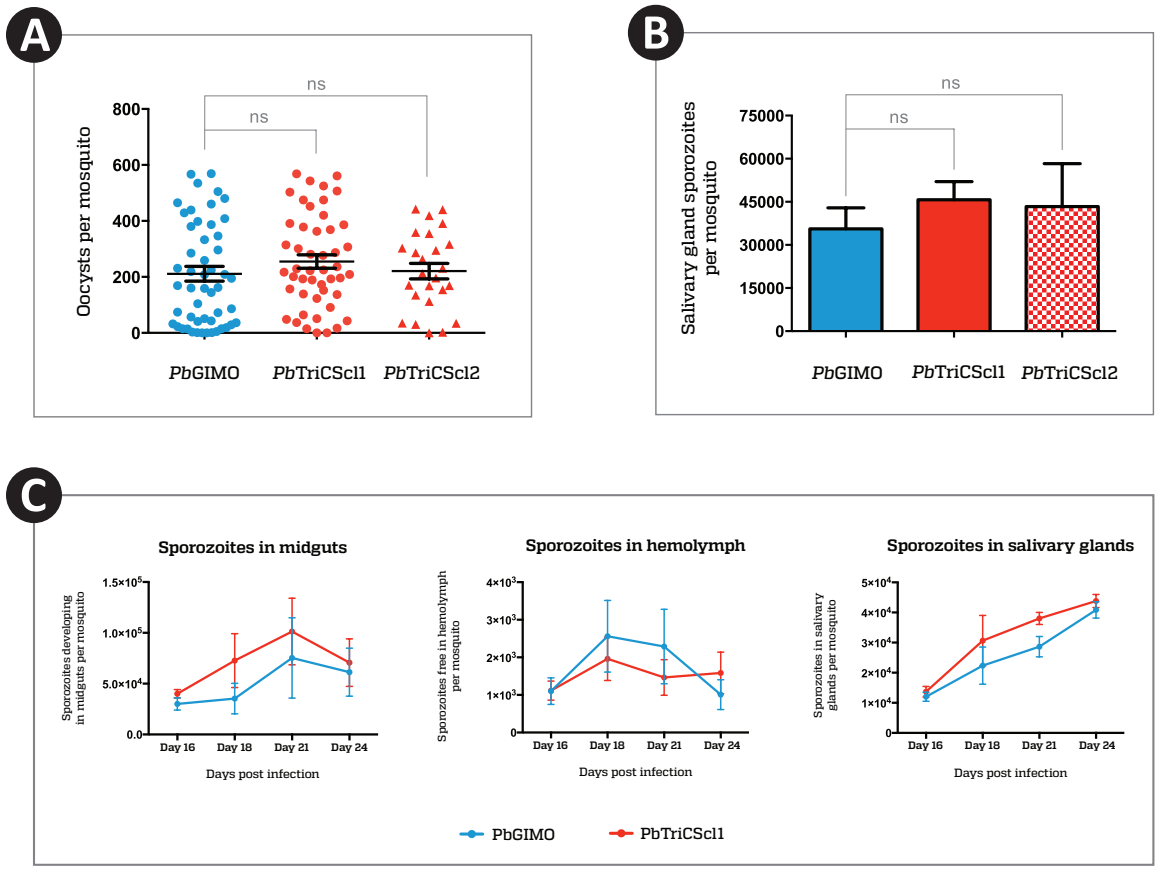

Figure 7: Sporogonic development of *Pb*TriCS
A- Number of oocysts in the mosquito midgut at day 12-13 post infection. **B-** Number of salivary glands sporozoites per mosquito at day 21 post infection. **C- (left)** Number of sporozoites developing within oocysts in the mosquito's midguts per mosquito; **(center)** Number of sporozoites free in the mosquito's hemolymph per mosquito; **(right)** Number of salivary glands sporozoites per mosquito; at days 16, 18, 21 and 24. Results are expressed as mean (bars) and standard error of the mean (error bars). Mann-Whitney non-parametric test was used between groups with a 95% confidence interval and there are no significant (ns) differences between *Pb*GIMO and *Pb*TriCS parasites (p>0,05).

Table 10: Number of sporozoites in midguts, hemolymph and salivary glands per mosquito at days 16, 18, 21 and 24 expressed as mean ± standard error of the mean.

Days post infection	Sporozoites in Midguts		Sporozoites in Hemolymph		Sporozoites in Salivary Glands	
	PbGIMO	PbTriCScl1	PbGIMO	PbTriCScl1	PbGIMO	PbTriCScl1
Day 16	30000 ± 6110,10	40000 ± 4163,33	1100 ± 353,84	1113,33 ± 254,12	12000 ± 1527,53	13666,67 ± 1763,83
Day 18	35333,33 ± 15025,90	72666,67 ± 26566,47	2560 ± 956,31	1960 ± 578,73	22333,33 ± 6173,42	30666,67 ± 8412,95
Day 21	75333,33 ± 39485,58	101333,33 ± 32768,54	2286,67 ± 990,51	1466,67 ± 475,58	28666,67 ± 3382,96	38000 ± 2000,00
Day 24	61333,33 ± 23673,70	70666,67 ± 23361,88	1006,67 ± 397,55	1586,67 ± 554,90	40873,33 ± 2722,75	43825 ± 2159,62

4.3 Gliding Motility of *Pb*TriCS parasites

After characterizing the sporogonic development of *Pb*TriCS parasites we started by assessing *Pb*TriCS gliding motility on a solid surface.We evaluated the gliding motility of *Pb*TriCS sporozoites, a mode of locomotion that is essential to sporozoite infectivity, where a circular movement may be observed on a solid surface. Experiments were performed by allowing 20.000 sporozoites of either *Pb*GIMO, *Pb*TriCScl1 (N=2) or *Pb*TriCScl2 to glide during one hour in a coverslip coated with one of various α-CS primary antibodies: 3D11 (α-*Pb*CS), 2A10 (α-*Pf*CS) and 2F2 (α-*Pv*CS) (Figure 8A).

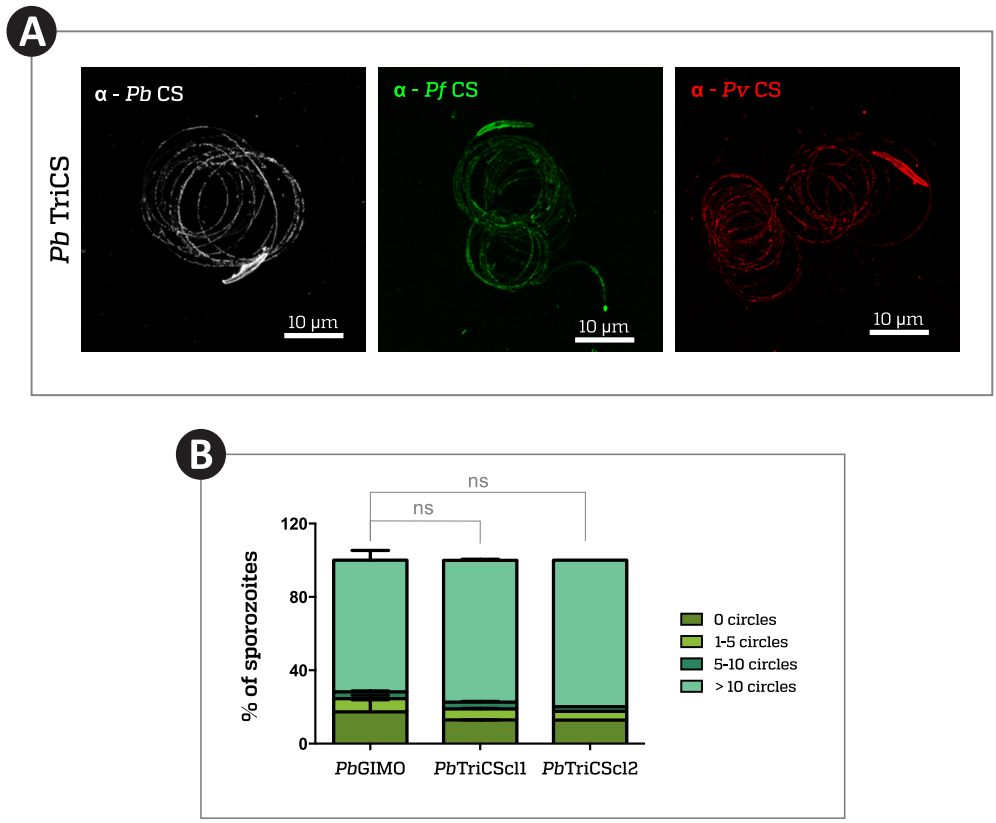

Figure 8: Gliding motility assay of *Pb*TriCS
A- Immunofluorescence microscopy images of *Pb*TriCS parasites gliding motility assay. As shown, *Pb*TriCS clones express the endogenous *P. berghei* CS protein as well as the CS proteins of *P. falciparum* and *P. vivax*; **B-** Results show the percentage of sporozoites that exhibit 0, 1-5, 5-10 or more than 10 circles. Bars indicate the mean of the percentage and error bars indicate de standard error of the mean. Two-way ANOVA was performed, demonstrating a non-significant (ns) statistical difference between *Pb*GIMO and *Pb*TriCS clones.

Concerning the CS protein expression and shedding during gliding, immunofluorescence images presented in Figure 8 show that *Pb*TriCS clones express the endogenous *P. berghei* CS protein as well as the CS proteins of *P. falciparum* and *P. vivax,* whereas *Pb*GIMO only expresses the *P. berghei* CS protein, as expected (not shown).

The number of circles corresponding to the shedding of CS protein by the parasite during gliding motility were counted by microscopy and the results indicate that most sporozoites were able to glide (*Pb*GIMO 82,7%; *Pb*TriCScl1 77,4%; *Pb*TriCScl2 79,9%) with a large majority gliding for more than 10 circles (*Pb*GIMO 71,8%; *Pb*TriCScl1 87,1%; *Pb*TriCScl2 87,2%) (Figure 8B).

4.4 Hepatic infectivity of *Pb*TriCS parasites

After characterizing the sporogonic development of *Pb*TriCS parasites and its gliding motility, we proceeded with the characterization of the hepatic development of *Pb*TriCS. For that end, we measured parasite infectivity and development by performing *in vitro* infections of Huh7 cells.

4.4.1 *In vitro* hepatic infectivity & development of *Pb*TriCS parasites

In order to evaluate the capacity of *Pb*TriCS to infect human hepatic cells, Huh7 human hepatoma cells cultured *in vitro* were infected with freshly dissected sporozoites of control *Pb*GIMO parasites, and of the transgenic *Pb*TriCScl1 and *Pb*TriCScl2 lines. Samples were collected from various biological replicates (N=4-5 for *Pb*GIMO & *Pb*TriCScl1; N=2-3 for *Pb*TriCScl2) at 24 and 48 hpi in order to determine the relative number of infected cells (24 and 48 hpi), as well as to quantify overall parasite development (48 hpi). Upon normalization to the *Pb*GIMO control, no statistically significant difference was observed between the infectivity of either *Pb*TriCS clone at either 24 or 48 hours post-infection in comparison the control parasites, (Figure 9A and 9B). The results expressed as mean of infection ± standard error of the mean are as follows: 1) 24hpi, *Pb*GIMO, 100 ± 5,1%, *Pb*TriCScl1, 109,9 ± 22%, *Pb*TriCScl2, 143,2 ± 52,4 %; 2) 48hpi, *Pb*GIMO, 100 ± 10,8%, *Pb*TriCScl1, 105,7 ± 19,8%, *Pb*TriCScl2, 132,6 ± 28,2%. Identical results were obtained when evaluating parasite development, with no statistically significant difference being observed between the size of control *Pb*GIMO and *Pb*TriCS clones at 48hpi (*Pb*GIMO: n=539, average area=249,2 ± 4,8 μm^2; *Pb*TriCScl1: n=489, average area=245,6 ± 5,2 μm^2 ; *Pb*TriCScl2: n=215, average area=240,3 ± 7,8 μm^2) (Figure 9C).

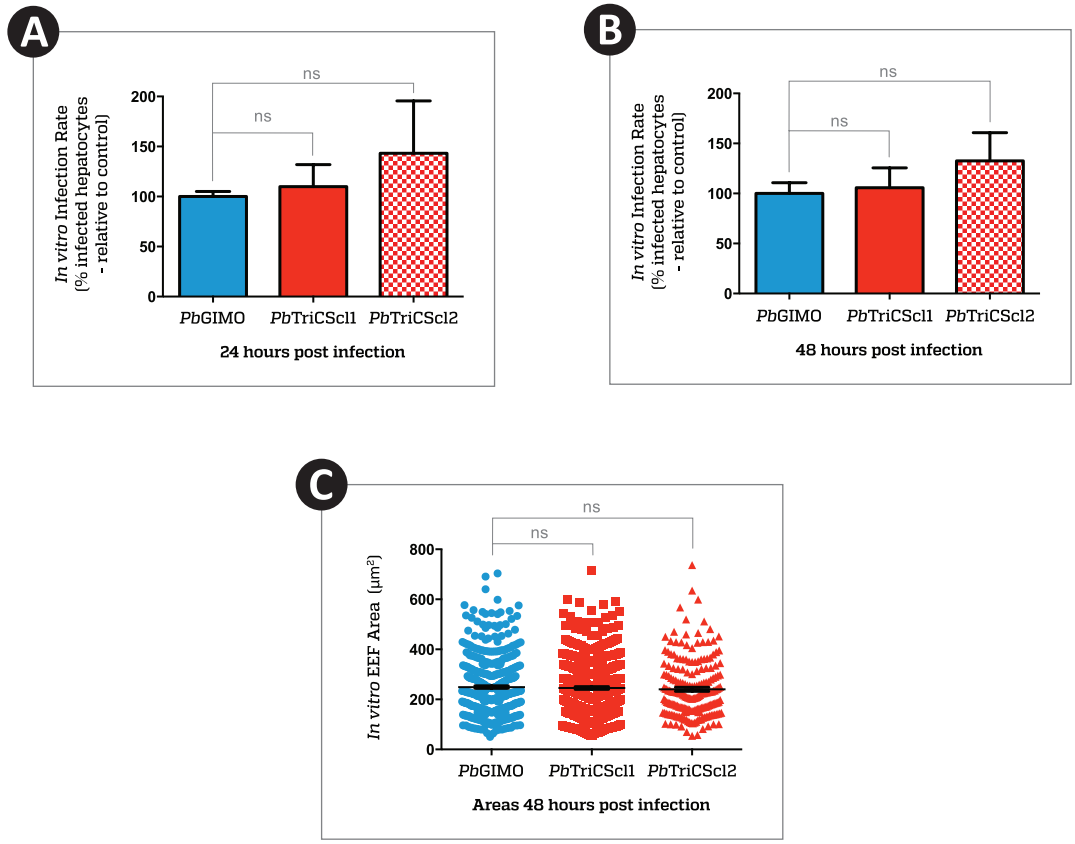

Figure 9: *Pb*TriCS infectivity and development in Huh7 in comparison with *Pb*GIMO parasites
A- Infection rate of *Pb*TriCS clones at 24 hours post-infection normalized to control *Pb*GIMO. **B-** Infection rate of *Pb*TriCS clones at 48 hours post-infection normalized to control *Pb*GIMO. **C-** Development of *Pb*TriCS clones at 48 hours post infection measured as EEF areas (μm^2). Results are expressed as mean (bars) and standard error of the mean (error bars). Mann-Whitney non-parametric test was used between groups with a 95% confidence interval and there are no statistically significant (ns) differences between *Pb*GIMO and *Pb*TriCS parasites (p>0,05).

4.4.2 *In vivo* hepatic infection of *Pb*TriCS parasites

Following the *in vitro* characterization of *Pb*TriCS parasites, we proceeded to evaluate *in vivo* the infectivity and development *Pb*TriCS parasites. For that end, C57BL/6J mice were infected by intravenous injection of sporozoites from either *Pb*GIMO (N=4 exp., n=12 mice), *Pb*TriCScl1 (N=4 exp., n=12 mice)) or *Pb*TriCScl2 (N=2 exp., n=7 mice). Infected livers were collected at 46 hours post-infection to measure parasite infectivity and development by immunofluorescence microscopy and qRT-PCR. Surprisingly, results showed statistically significant reduction of 50-60% in overall parasite load as measured by qRT-PCR, between mice infected with both of the *Pb*TriCS clones and control *Pb*GIMO infected mice (*Pb*GIMO: 100 ± 12,1%; *Pb*TriCScl1: 46,9 ± 12,3%; *Pb*TriCScl2: 34,5 ± 15,8%). (Figure 10)

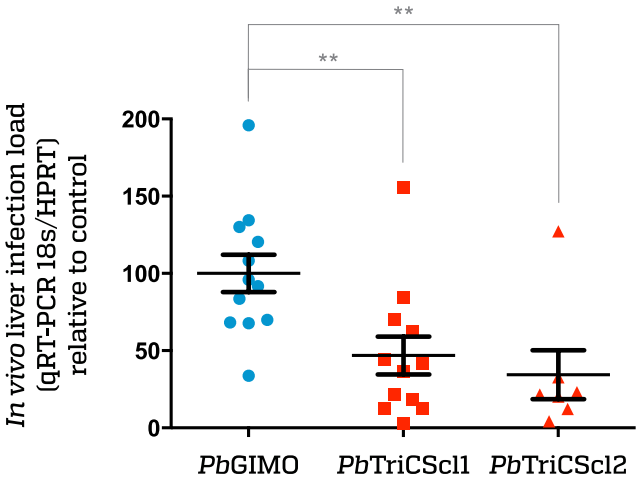

Figure 10: *In vivo* liver *Pb* infection load measured by qRT-PCR
Results are expressed as the mean of *Pb* infection load and error bars represent the standard error of the mean. Mann-Whitney non-parametric test identified statistically significant differences for both clones (P≤0.01).

To further characterize the observed reduction in infection load, the infection rate was determined by assessing the average number of EEFs by liver area (EEFs/mm^2 of liver). The results show a statistically significant difference (P≤0.01) between the infection rate of the *Pb*TriCScl2 clones (*Pb*GIMO: 100 ± 13,3 EEFs/mm^2; *Pb*TriCScl1: 68,2 ± 16,1 EEFs/mm^2; *Pb*TriCScl2, 47,8 ± 18,7 EEFs/mm^2;Figure 11A), indicating that overall there is a smaller number of parasite *Pb*TriCS being able to establish a successful liver infection when compared to control *Pb*GIMO parasites.

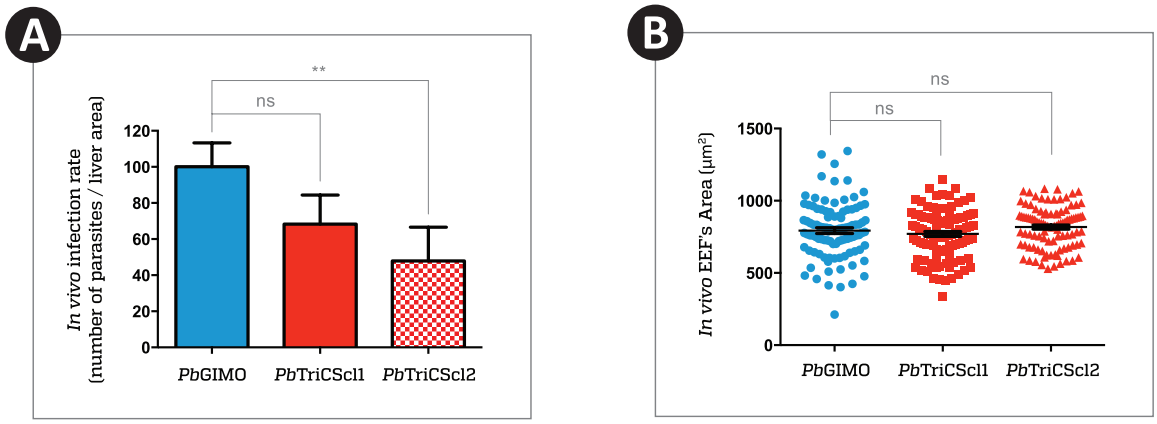

Figure 11: *In vivo* infectivity and development of *Pb*TriCS
A- *In vivo* infectivity determined by the number of EEFs by liver area (mm^2). Results are expressed as the mean of the number of EEFs/mm^2 ± standard error of the mean (error bars). Mann-Whitney test revealed a ** statistical significant difference (P≤0.01) between *Pb*GIMO and *Pb*TriCScl2 and no statistical significant difference between *Pb*GIMO and *Pb*TriCScl1 (p>0.05). **B-** *In vivo* development determined by measuring the areas of EEFs (µm^2). Results are expressed as mean area of EEF (µm^2) ± standard error of the mean (error bars). Mann-Whitney non-parametric test was used between groups with a 95% confidence interval and there are no significant (ns) differences between *Pb*GIMO and *Pb*TriCS parasites (p>0,05).

Nonetheless, analysis of parasite development by measurement of their overall size indicates that there is no compromise in the parasite ability to complete its development (*Pb*GIMO: n=100 EEFs, average size=793,2 ± 19,5 μm^2; *Pb*TriCScl1: 100 EEFs, average size=770,1 ± 17,0 μm^2; *Pb*TriCScl2: n=100 EEFs, average size=817,5 ± 14,3 μm^2; Figure 11B).

4.4.3 *In vitro* & *In vivo Pb*TriCS protein expression

In order to assess protein expression in *Pb*TriCS, antibodies against the *Pb*UIS4, *Pb*CS, PfCS and PvCS proteins where used to stain parasites developing inside infected human hepatoma cultured *in vitro* at 24 and 48 hpi and *in vivo* inside mouse hepatocytes at 48hpi.
As shown in Figures 12 and 13, all parasites assessed express UIS4, which was used in this experiment as a general marker for the parasite, allowing to observe the parasite PVM even if any of the CS proteins are not stained. Our results show that both clones express all CS in their genome: endogenous *Pb*CS and exogenous PfCS and PvCS. In *Pb*GIMO, as expected, it is only possible to observe *Pb*CS expression.

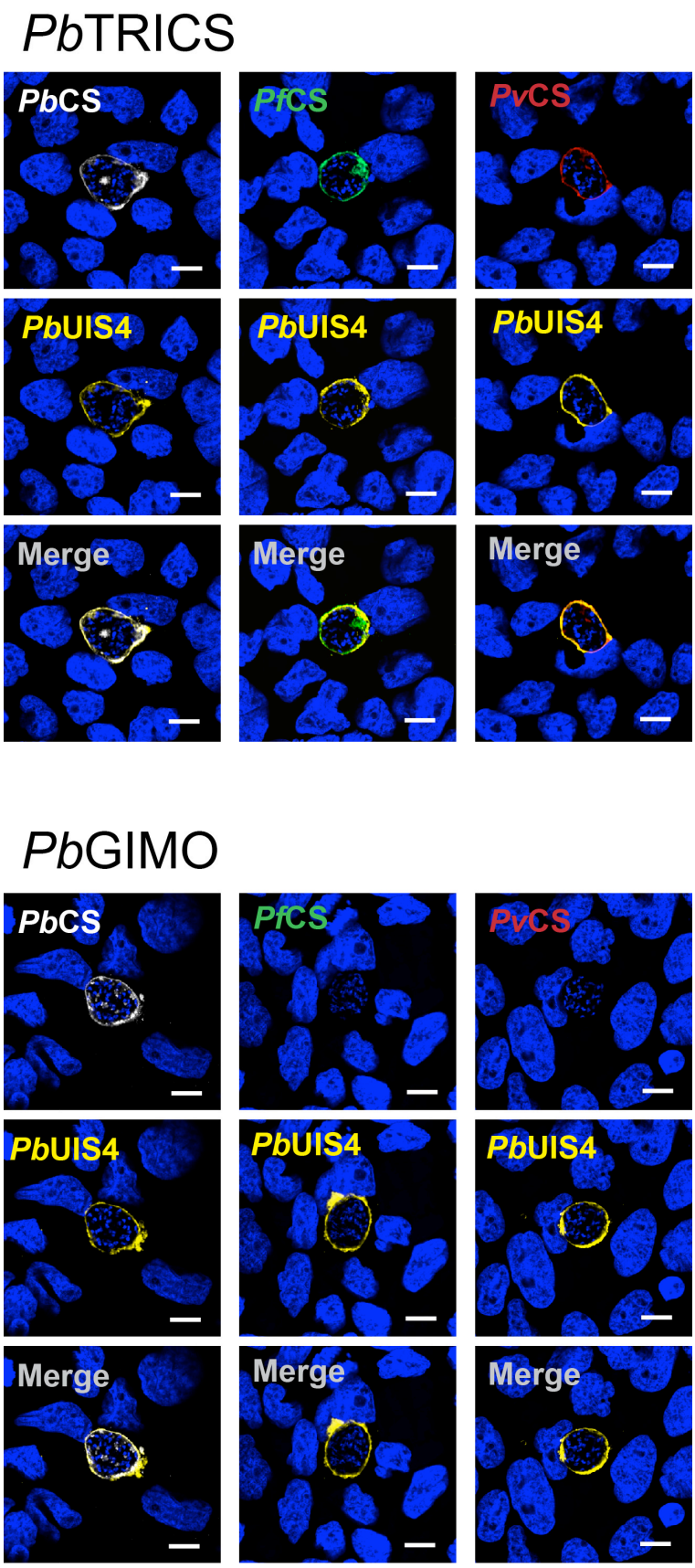

Figure 12: Immunofluorescence microscopy of EEFs in Huh7 hepatoma cell line at 48 hours post-infection
Scale bar: 10µm

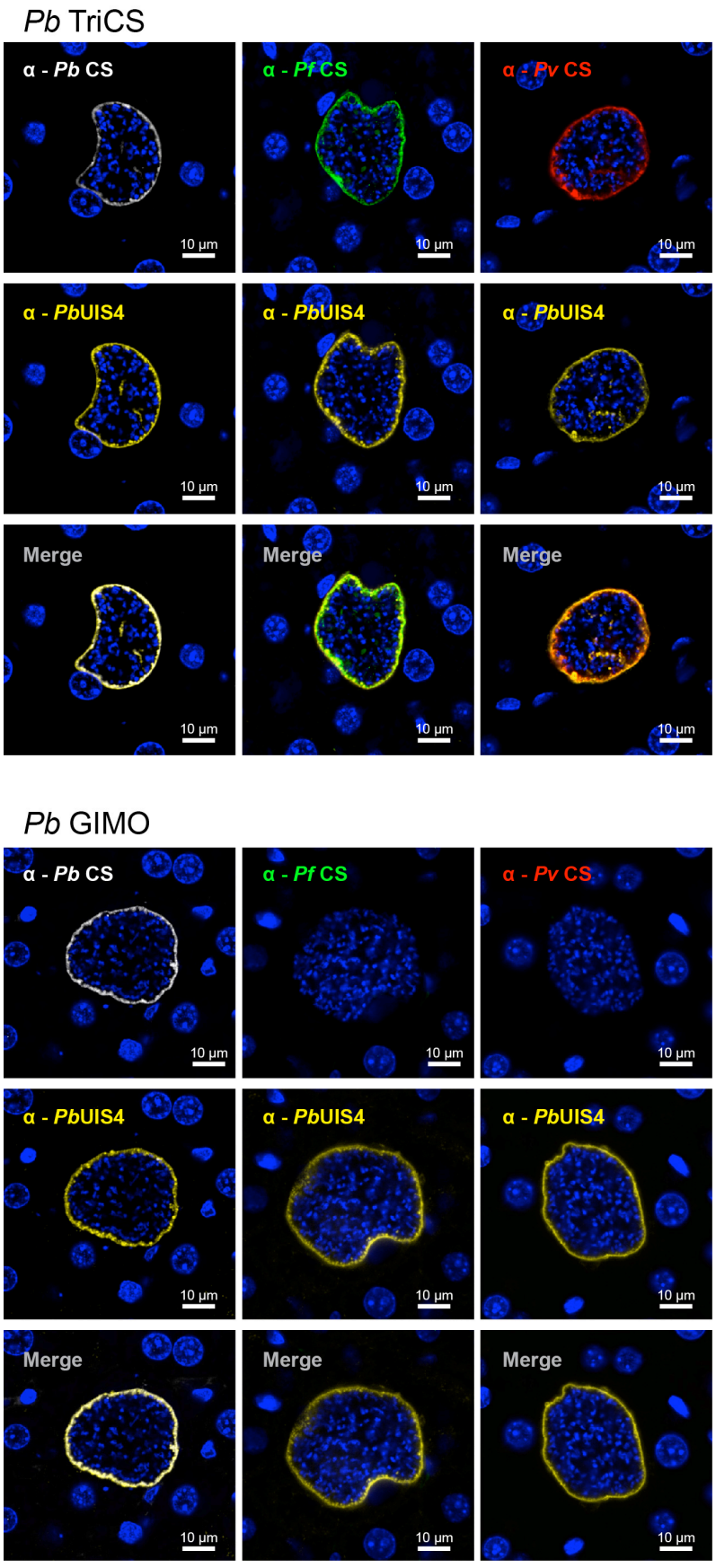

Figure 13: Immunofluorescence microscopy of EEFs in C57BL/6J mice livers at 46 hours post-infection

4.5 Cell Traversal Ability of *Pb*TriCS Parasites

Since the *in vivo* results show that *Pb*TriCS is not capable of infect the mouse liver in equal measure as *Pb*GIMO, we decided to further explore the potential cause of such difference by performing an *in vitro* cell traversal assay. After infection, sporozoites enter the blood stream and eventually reach the host liver where they cross the liver sinusoids, fenestrated blood vessels lined with endothelium and Kupffer cells (liver-resident macrophages), and traverse several hepatocytes by a process of migration known as cell traversal where they disrupt hepatocytes plasma membrane without infecting them.[15]

We employed a flow cytometry based assay to quantify the percentage of cells traversed by sporozoites during infection of human hepatoma cells in vitro. This assay allows the specific quantification of cells that retain fluorescent FITC-Dextran in their interior upon parasite transversal. The results show that *Pb*TriCS clones are not capable of traversing cells to the same extent of the wild-type *Pb*GIMO, as only 50,3 ± 3,2% or 61,2 ± 2,3% of cells incubated with *Pb*TriCScl1 or *Pb*TriCScl2, respectively, appear to be traversed, when normalized to the total amount of cells traversed upon incubation with *Pb*GIMO parasites (100 ± 1,3%) (Figure 14).

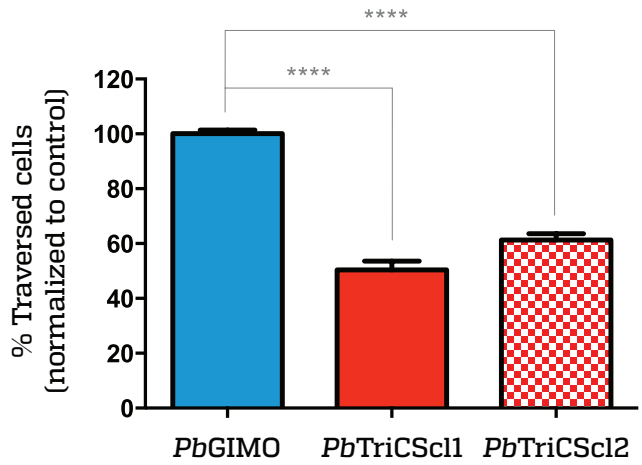

Figure 14: FACS analysis of the percentage of traversed cells, normalized to control. Results are expressed as mean of traversed cells ± standard error of the mean (error bars). Mann-Whitney test revealed a **** statistical significant difference (P≤0.0001) between *Pb*GIMO and *Pb*TriCS clones.

4.6 The impact of cell traversal deficiency on *in vivo* hepatic infection

4.6.1. Infection of macrophage depleted mice

Previously Ishino *et al.,* reported a sporozoite microneme protein essential for cell traversal (SPECT) by *Plasmodium* parasites. Parasites with whose *spect* gene is disrupted have *in vivo* liver infectivity reduced as they completely lack cell traversal capacity, but they are able to normally invade and infect cells *in vitro.* Although these *spect* mutants completely lack cell

traversal ability, they are able to infect hepatocytes *in vivo* when Kupffer cells were depleted. The authors propose that macrophage depletion creates gaps between endothelial cells that allow *spect* mutant sporozoites to reach hepatocytes by gliding motility only, restoring the wild-type phenotype in *spect* mutants. [69]

Once *Pb*TriCS exhibits, to some extent, a similar phenotype as *spect* mutants, we decided to deplete macrophages in order to assess if in the absence of these cells, *Pb*TriCS infectivity *in vivo* was restored.

In order to deplete macrophages, C57BL/6J mice were treated with clodronate delivered to cells through liposomes, which accumulates in macrophages leading to cell apoptosis.[70] Mice were either treated via i.v.. injection with clodronate + liposomes or with PBS + liposomes, used as a control and subsequently infected with 30.000 sporozoites of *Pb*TriCScl1. 46 hours post infection livers were collected and qRT-PCR was performed in order to analyze macrophage depletion and *Pb* infection load (Figure 15).

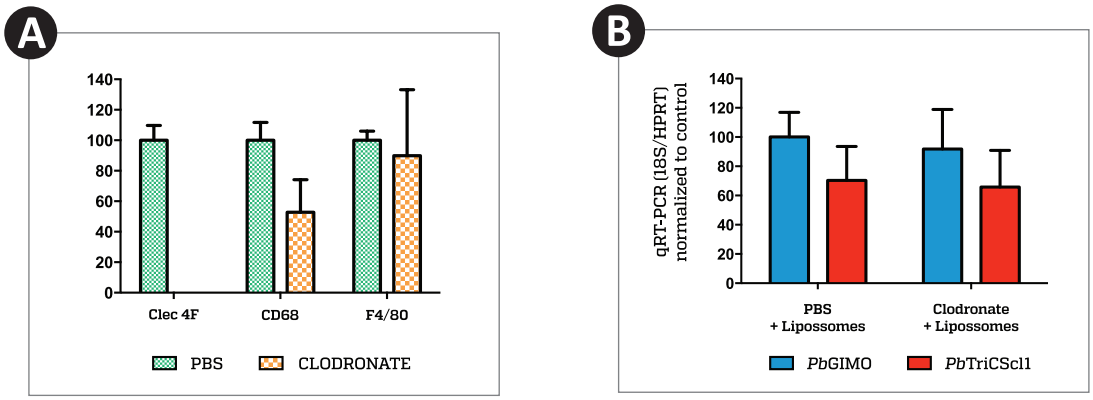

Figure 15: Macrophage depletion and infection load at 46 hours post-infection
A- Macrophage depletion detected by qRT-PCR by gene expression of Clec 4F (Kupffer cell receptor) and CD68 and F4/80 (Kupffer cell marker). **B-** *Pb* liver infection load measured by qRT-PCR between the two parasites (*Pb*GIMO and *Pb*TriCScl1) and between the two treatments (PBS + liposomes or clodronate + liposomes).

To assess the efficiency of macrophage depletion, 3 genes were analyzed: Clec4F (Kupffer cell receptor) and CD68 and F4/80 (Kupffer cell markers).[71] Our results indicate that macrophage depletion was successful as results upon normalization to gene expression in mice treated with PBS + liposomes are as it follows: Clec4F in mice treated with PBS + liposomes: 100 ± 9,7; Clec4F in mice treated with clodronate + liposomes: 0,03 ± 0; CD68 in mice treated with PBS + liposomes: 100 ± 11,7; CD68 in mice treated with clodronate + liposomes: 52,8 ± 21,4; F4/80 in mice treated with PBS + liposomes: 100 ± 6,0 ; F4/80 89,9 ± 43,3 (Figure 15A).

However, infection load, as a ratio measure of *P. berghei* 18 S rRNA gene expression to the mouse HPRT gene expression normalized to *Pb*GIMO infection in mice treated with PBS + liposomes, show that macrophage

depletion was not sufficient to revert the wild-type phenotype, as *Pb*TriCScl1 was not able to establish a liver infection to the same extent as *Pb*GIMO. Results are as it follows: 3 *Pb*GIMO infected mice treated with PBS + liposomes: 100 ± 16,9; 3 *Pb*GIMO infected mice treated with clodronate + liposomes: 91,8 ± 27,1; 4 *Pb*TriCScl1 infected mice treated with PBS + liposomes: 70,3 ± 23,3; and 4 *Pb*TriCScl1 infected mice treated with clodronate + liposomes: 65,8 ± 25 (Figure 15B).

4.6.2 Early liver infection

Given that the macrophage depletion was not successful, we decided to perform an experiment to assess if the *Pb*TriCS parasite was able to reach and invade the liver similarly to *Pb*GIMO. To accomplish that, mice were infected with $3x10^4$ sporozoites, either *Pb*GIMO or *Pb*TriCScl2 and livers were collected to measure *Pb* infection load was measured by qRT-PCR. Results showed statistically significant reduction of 40-50% in overall parasite load as measured by qRT-PCR, between mice infected with *Pb*TriCScl2 and control *Pb*GIMO infected mice (*Pb*GIMO: 100 ± 10,1%; *Pb*TriCScl2: 43,9 ± 9,8%). (Figure 16)

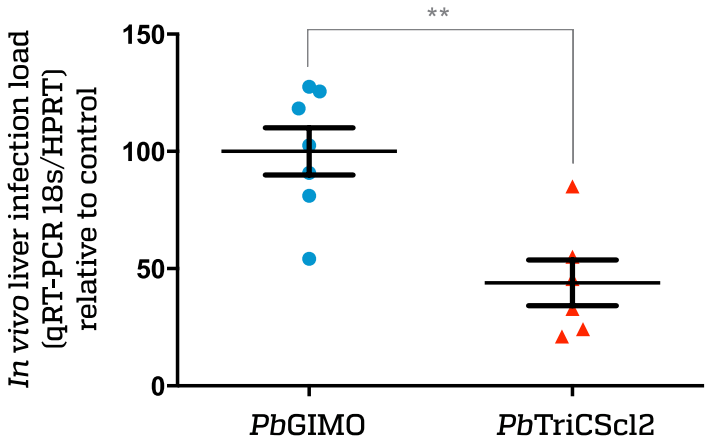

Figure 16: *In vivo* liver *Pb* infection load at 6 hours post-infection measured by qRT-PCR.
Results are expressed as the mean of *Pb* infection load and error bars represent the standard error of the mean. Mann-Whitney non-parametric test determined statistical significant differences between *Pb*GIMO and *Pb*TriCScl2 (P≤0.01).

4.7 Humoral responses elicited by immunization with *Pb*TriCS

Following the immunization protocol thoroughly described in Materials & Methods, we employed ELISA to measure the levels of antibodies in the sera of *Pb*TriCS-immunized mice. The wells of the plate were coated with peptides from the antigen of interest (either *P. berghei, P. falciparum* or *P. vivax* CS protein) and the wells were then filled with serial dilutions of the mouse serum.

As shown in Figure 17, the antibodies present in the serum from *Pb*TriCS-immunized mice are able to recognize PfCS and PvCS peptides and the IgG titers of those antibodies are similar to those of the antibodies raised against *Pb*CS peptides. As expected, mock immunized mice sera does not have the antibodies able to recognize any of the CS peptides and *Pb*GIMO immunized mice antibodies are only able to recognize *Pb*CS peptides.

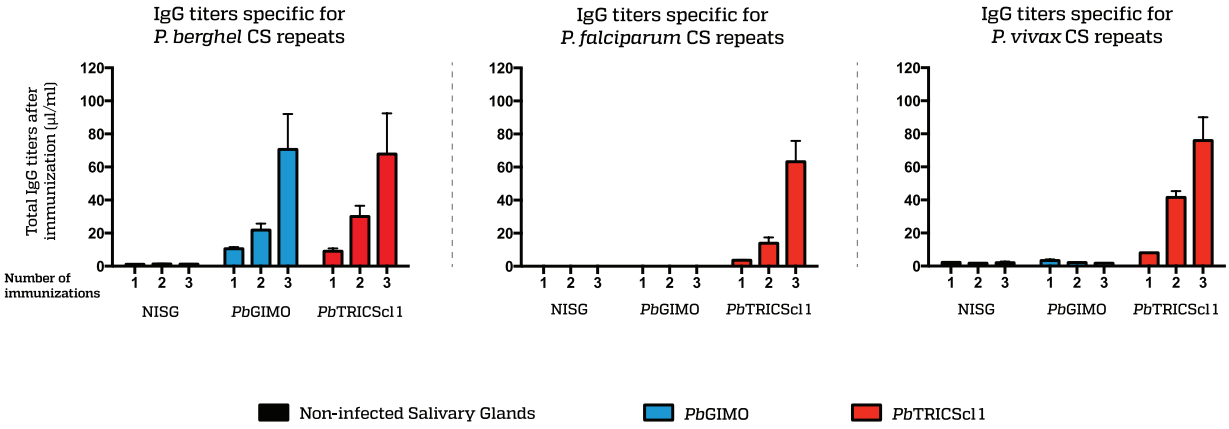

Figure 17: Humoral responses assessed by ELISA determination of IgG titer for CS repeats in mouse sera collected after 1, 2 and 3 immunizations.
Results are expressed as mean of the IgG titers after immunizations (µl/ml) and error bars represent the standard error of the mean.

DISCUSSION

5

5. Discussion

Malaria was responsible for more than half-million deaths in 2014. Unfortunately, no vaccine against this devastating disease has yet been licensed.[1] RTS,S is the most advanced malaria vaccine candidate to date. It is a subunit pre-erythrocytic malaria vaccine candidate that elicits immune responses against *P. falciparum* CS protein. However, results from large-scale phase 3 clinical trials in Africa have shown modest results in vaccine efficacy (around 30%) and have further shown that this efficacy wanes over time. [33] On the other hand, whole-organism pre-erythrocytic (WOPE) malaria vaccines have been shown to be the sole malaria vaccination strategy capable of conferring sterile immunity against human *Plasmodium* species in naïve volunteers. WOPE malaria vaccines were shown to elicit potent CD8+ T cell responses. Nevertheless, current WOPE vaccination approaches rely on the use of human infective *Plasmodium* sporozoites, which, among other limitations, present a risk of symptomatic infection if a breakthrough event occurs.

To tackle obstacles presented by WOPE vaccines, the Prudêncio Lab proposes a different vaccination approach. The idea is that genetically modified *P. berghei* parasites can be used as a platform to deliver immunogens of human-infective *Plasmodium* parasites, eliciting strong protective responses against these parasites, without the risk of clinical manifestation of malaria as the rodent malaria parasites are unable to replicate inside human red blood cells. Previous studies performed in the Prudêncio Lab with a transgenic *P. berghei* expressing *P. falciparum* CS protein under the control of *P. berghei* UIS4 promoter (*Pb*(*Pf*CS@UIS4)) showed that this parasite not only infects and develops in liver cells *in vitro*, *ex vivo* and *in vivo*, but is also capable of eliciting both humoral and cellular immune responses against *P. falciparum*, establishing a proof-of-concept for this vaccination strategy.

The work developed in this Master's thesis aimed at characterizing a newly generated *Pb*TriCS parasite line, a *P. berghei* parasite that simultaneously expresses *P. falciparum* CS and *P. vivax* CS, in addition to the endogenous *P. berghei* CS. We hypothesized that this new parasite may constitute a versatile vaccine candidate capable of simultaneously eliciting protection against these two major human malaria parasites.

In order to characterize *Pb*TriCS throughout its life cycle, we started with an in-depth analysis of its mosquito stage development. By evaluating the number of oocysts, the number of sporozoites developing inside the oocysts, the number of sporozoites free in the hemolymph, and the number of sporozoites present in the salivary glands at different time points, we were able to conclude that the fitness of *Pb*TriCS throughout its entire mosquito stage development is similar to that of control *Pb*GIMO parasites (Figure 7). Since the proposed vaccination approach relies on the use of fully infective sporozoites, a normal mosquito development is essential for vaccine production. Previous studies showed that the replacement of the *Pb*CS gene

by the *Pf*CS gene in *P. berghei* may lead to the impairment of parasite development that results in a considerably reduced the number of salivary glands infective sporozoites. [65] Unpublished data from the Prudêncio Lab confirmed that *P. berghei* sporozoites where the *Pb*CS gene was replaced by the *Pf*CS gene were able to produce the same number of oocysts but were not able to invade the salivary glands to the same extent as wild-type sporozoites since the sporozoites remained free in the mosquito's hemolymph. However, having two CS proteins inserted in non-essential loci and preserving the *Pb*CS gene intact has overcome this problem. Moreover, we have shown that all three CS proteins are being expressed as expected and are shed during gliding motility (Figure 8). It is very well demonstrated that high titers of anti-CS antibodies are essential to mount a protective response against a new infection, therefore the fact that CS proteins are being correctly expressed and shed by the sporozoites during gliding may promote protection warranties that the protein is available to be processed by the immune system and possible induce the required high titers of antibodies.

We further characterized the hepatic infectivity of *Pb*TriCS parasites by performing *in vitro* studies using a human hepatoma cell line – Huh7. No differences in parasite infection and development were observed for two independent *Pb*TriCS clones in comparison with control *Pb*GIMO parasites (Figure 9).Our data also shows that all three CS proteins are being properly translocated and expressed on the PVM, as shown by immunofluorescence microscopy (Figure 12).

Following the *in vitro* characterization of *Pb*TriCS hepatic infectivity, we subsequently infected C57BL/6J mice to evaluate parasite's liver infectivity *in vivo*. Our results did not fully reproduce the phenotype observed *in vitro* since the liver infection load measured by qRT-PCR was significantly lower in *Pb*TriCS-infected mice when compared to control *Pb*GIMO-infected animals (Figure 10). To try and understand the cause of this difference in infection load, we used immunofluorescence microscopy to evaluate whether this was due to a reduction on the number of parasites establishing an infection was lower in PbTriCS infected animals than in control animals or if the development of the PbTriCS parasite was impaired. Our results are unclear regarding infection rate, since *Pb*TriCScl2 is statistically significantly lower than control *Pb*GIMO, whereas *Pb*TriCScl1 is not. Yet, no statistically significant difference was observed in *Pb*TriCS development when compared to control *Pb*GIMO (Figure 11). Therefore, we believe our differences in infection load to be a result of a lower number of parasites being able to establish a liver-stage infection. Importantly, all *Pb*TriCS parasites that are capable of establishing an *in vivo* liver infection express the endogenous *Pb*CS as well as both engineered CS proteins, *Pf*CS and *Pv*CS, as can be observed by microscopy (Figure 13). Moreover, all proteins are being correctly translocated and expressed on the PVM. Since it has been shown that late liver stage-arresting parasites induce higher $CD8^+$ T cell responses [72], it is important that *Pb*TriCS development is not impaired and that it is able to fully express the antigens required to elicit an immune response against a subsequent sporozoite challenge.

Our hypothesis that *Pb*TriCS's lower infection load measured by qRT-PCR was due to lower number of parasites present in the liver was confirmed by cell-traversal assay results performed *in vitro.* Our results clearly indicate that *Pb*TriCS is not able to traverse cells with the same efficacy as control *Pb*GIMO parasites (Figure 14).

We then aimed to indirectly link the in vivo reduction of *Pb*TriCS infection to the impaired capacity for these parasites to transverse cells by two distinct approaches. First, we followed a premise based, on the studies of Ishino *et al.* [69] which indicate that macrophage depletion may facilitate the migration of sporozoites to the liver, increasing infection by allowing parasites to establish infection without having to rely so heavily in their ability to transverse. We carried out a liver macrophage depletion experiment, followed by sporozoite injection. Unfortunately the results of this experiment were inconclusive, as *Pb* liver infection load was reduced in clodronate + liposomes treated mice infected either with *Pb*GIMO or *Pb*TriCS parasites when compared with PBS + liposomes treated (Figure 15). Nonetheless, approximately 50% of the *Pb*TriCS parasites were able to establish a normal liver infection and most parasites seem to achieve full development.

Secondly, we aimed to quantify the number of parasite that are able to initiate infection by collecting infected livers with both parasites shortly after inoculation, clearly decoupling parasite capacity to establishing infection that is directly related to their capacity to transverse cells from parasite development inside an infected liver cell, Our qRT-PCR results show a lower *Pb* infection load between *Pb*GIMO and *Pb*TriCScl2, which agrees with the hypothesis that the lower parasite load observed results from a lower number of parasites being able to establish a liver infection (Figure16).

The *Pb*TriCS parasite was generated and characterized as a possible vaccine candidate. Therefore, immunological studies are necessary to whether this vaccination strategy can elicit immune responses against *Pb*CS, *Pf*CS and *Pv*CS. An ELISA assay performed using CS peptides as antigen showed that although *Pb*TriCS has a lower ability to infect the liver, a standard three immunizations protocol is enough to elicit the same humoral responses against *Pb*CS as *Pb*GIMO. As *Pb*CS is a shared CS protein between *Pb*GIMO and *Pb*TriCS, IgG titers against PbCS can be employed to compare the humoral responses elicited by immunizations with *Pb*GIMO or *Pb*TriCS. As shown by ELISA (Figure 17), IgG titers against *Pb*CS present in the serum from immunized mice are similar between *Pb*GIMO and *Pb*TriCS. Furthermore, we demonstrated that the antibodies present in the serum from *Pb*TriCS-immunized mice is able to recognize both PfCS and PvCS peptides since our ELISA assay revealed high titers of IgG against them and these IgG titers are similar to those of antibodies against *Pb*CS peptides.

It was reported in 2014 that only 2 *P. vivax* vaccine candidates were in Phase I clinical trials (PvDBP – *Pv* Duffy Binding Protein; and PvCSP – *Pv* CS protein) whereas there were a total of 23 *P. falciparum* vaccine candidates (including RTS,S in Phase III clinical trials). [73] Most malaria-endemic countries outside of Africa have co-transmission of both *P. falciparum* and *P. vivax*. If there is a licensed vaccine against *P. falciparum* administered in areas of co-

transmission, an increase in *P. vivax* malaria infections is expected to occur. [8] For this reason, and in agreement with the World Health Organization Malaria Vaccine Technology Roadmap guidelines, a malaria vaccine against both *P. falciparum* and *P. vivax* should be licensed by 2030. [24]

The *Pb*TriCS parasite is a good alternative to current vaccine candidates since it overcomes the safety concerns that are present in human infective sporozoites as a vaccination strategy. Moreover, we have shown that it is able to elicit humoral responses against both *P. falciparum* and *P. vivax* CS peptides. Nevertheless, there are various questions that remain unanswered and further experiments should be performed in order to validate this parasite as good WOPE malaria vaccine candidate. Some of which are discussed below:

- First, since the *Pb*TriCS parasite has lower cell traversal ability than *Pb*GIMO parasites, the decrease in liver infection should be evaluated with different inoculation protocols. It has been shown that routes of administration different from i.v. or mosquito bite, such as intradermal or subcutaneous injection, lead to suboptimal immunogenicity and protective efficacy. [44] In 2014, 78% of deaths reported by malaria were in children under the age of five [1] which makes them the principal target of a malaria vaccine. Therefore, a route of vaccine delivery different from i.v. is highly desirable. To tackle these obstacles, experiments in animal models should be performed in order to elucidate if increasing the number of sporozoites used in intradermal or subcutaneous injection may trigger immune responses similar to i.v. inoculation of sporozoites.
- Second, although antibody responses are powerful at reducing the number of parasites able to establish a liver infection, high antibody titers are required in order to be effective.[74] $CD8^+$ T cells specific for parasite-derived peptide/class I MHC molecule complexes on infected hepatocytes surface are thought to be the primary immune effectors responsible for eliminating parasites that invade and replicate within hepatocytes by the release of interferon-gamma (IFN-γ) by $CD8^+$ T cells activation.[74] [75] [76] Cellular immune responses triggered by *Pb*TriCS parasites could be evaluated using an immunization protocol similar to the one used in this Master's project, where 3 immunizations with *Pb*TriCS parasites followed by chloroquine treatment were performed. Using a protocol similar to the one described by Nganou-Makamdop *et al.,* it is possible to evaluate by flow-cytometry analysis what kind of cellular immune responses are being triggered by *Pb*TriCS immunization.[77]
- Third, to evaluate if the serum from *Pb*TriCS-immunized mice is able to recognize and block infection by *P. falciparum* and *P. vivax* sporozoites 3 experiments may be performed. In order to assess binding affinity to *P. falciparum* and *P. vivax* sporozoites, IFAT (immunofluorescence antibody test) could be used to detect antibodies in immune sera following a protocol using *P. falciparum* and *P. vivax* sporozoites immobilized on a glass slide and incubated with the serum of mice immunized with *Pb*TriCS. If antibodies against antigens on the surface of either *P. falciparum* or *P. vivax* sporozoites are present in the serum,

they will bind to these antigens on the sporozoites. These antigen-bound antibodies are detected by the use of a secondary antibody, anti-mouse, that has been conjugated to a fluorochrome in an immunofluorescence microscopy protocol similar to the one used in this master's project. This assay enables assessing the ability of the serum from the mice immunized with *Pb*TriCS to recognize and bind to *P. falciparum* and *P. vivax* sporozoites.

- Fourth, to assess the ability of the sera from immunized mice to block infection, a gliding motility assay where *P. falciparum* or *P. vivax* sporozoites are pre-incubated with IgG from *Pb*TriCS-immunized mice can be used, employing a protocol similar to the one used by Behet *et al.,* where sporozoite trails are counted by immunofluorescence microscopy.[78] If the serum from immunized mice recognizes the *P. falciparum* and *P. vivax* sporozoites, it is expected that these parasites will exhibit fewer trails since the immune serum is able to inhibit gliding motility. Live microscopy could also be performed on a gliding assay protocol in order to be able to demonstrate if the *Pb*TriCS immunized mouse serum is able to inhibit the gliding motility in *P. falciparum* and *P. vivax* sporozoites using the DIC (differential interference contrast) microscopy technique.
- Fifth, in 2013, March *et al.,* showed that *P. falciparum* is able to fully complete its liver stage development in micropatterned co cultures of human primary hepatocytes amongst stromal cells, including the release of infected merozoites, while *P. vivax* is able to establish late liver stage development. [79] Therefore, using these human primary hepatocytes it is possible to assess whether *Pb*TriCS is able to block infection of *P. falciparum* and *P. vivax* during liver stage development. By incubating human primary hepatocytes with serum samples from *Pb*TriCS immunized mice and subsequently infecting these human primary hepatocytes with *P. falciparum* and *P. vivax* we can assess invasion, infectivity and development of both parasites in the presence of serum-incubated hepatocytes and hepatocytes cultured in normal medium. If humoral/ cellular responses triggered by an immunization with *Pb*TriCS parasite are able to block *P. falciparum* or *P. vivax* infection in human liver, infectivity and development of these parasites should be decreased in human primary hepatocytes incubated with sera from *Pb*TriCS-immunized mice.

  Sixth, since the vaccination strategy is based on infective, live salivary glands sporozoites, efforts should be made towards designing a protocol similar to the one used by Sanaria™ for PfSPZ, in order to purify and cryopreserve *Pb*TriCS sporozoites that are able to infect and develop within hepatocytes without having its infectivity reduced by cryopreservation.

Despite the fact that the *Pb*TriCS parasite seems to be less able to establish an *in vivo* liver stage in comparison with *Pb*GIMO parasites, this could be easily solved on the context of vaccination by increasing the number of sporozoites delivered upon vaccination. Considering that this defect is specific for cell traversal and not prior or after this stage and that our data shows that there is no reduced fitness in the sporogonic development by *Pb*TriCS, we do

not see any obstacle in producing higher number of parasites in the mosquito stages to fulfill the need of delivering a higher number of parasites.

Most importantly, no defects were later found on development, implying that the parasites that are able to establish a liver infection express both the antigens introduced by genetic modification. This suggests that this parasite constitutes a good tool to study protection against *P. falciparum* and *P. vivax* parasites. Further studies should be performed in order to fully validate *Pb*TriCS as a vaccine candidate against the two major species of human-infective *Plasmodium*.

REFERENCES

6

6. REFERENCES

1. WHO. World Malaria Report 2014. (2014). at <http://www.who.int/malaria/publications/world_malaria_report_2014/report/en/>

2. Sachs, J. & Malaney, P. The economic and social burden of malaria. *Nature* **415,** 680–5 (2002).

3. Jones, M. K. & Good, M. F. Malaria parasites up close. *Nat. Med.* **12,** 170–1 (2006).

4. Prudêncio, M., Mota, M. M. & Mendes, A. M. A toolbox to study liver stage malaria. *Trends Parasitol.* **27,** 565–74 (2011).

5. White, N. J. Determinants of relapse periodicity in Plasmodium vivax malaria. *Malar. J.* **10,** 297 (2011).

6. Guerra, C. a. *et al.* The international limits and population at risk of Plasmodium vivax transmission in 2009. *PLoS Negl. Trop. Dis.* **4,** (2010).

7. Price, R. N. *et al.* Vivax malaria: neglected and not benign. *Am. J. Trop. Med. Hyg.* **77,** 79–87 (2007).

8. Herrera, S., Corradin, G. & Arévalo-Herrera, M. An update on the search for a Plasmodium vivax vaccine. *Trends Parasitol.* **23,** 122–128 (2007).

9. Mendes, C. *et al.* Duffy negative antigen is no longer a barrier to Plasmodium vivax--molecular evidences from the African West Coast (Angola and Equatorial Guinea). *PLoS Negl. Trop. Dis.* **5,** e1192 (2011).

10. Miller, L. H., Mason, S. J., Clyde, D. F. & McGinniss, M. H. The resistance factor to Plasmodium vivax in blacks. The Duffy-blood-group genotype, FyFy. *N. Engl. J. Med.* **295,** 302–4 (1976).

11. Miri-Moghaddam, E., Bameri, Z. & Mohamadi, M. Duffy blood group genotypes among malaria Plasmodium vivax patients of Baoulch population in southeastern Iran. *Asian Pac. J. Trop. Med.* **7,** 206–207 (2014).

12. Hedrick, P. W. Population genetics of malaria resistance in humans. *Heredity (Edinb).* **107,** 283–304 (2011).

13. White, N. J. *et al.* Malaria. *Lancet* **383,** 723–735 (2014).

14. Reyes-Sandoval, A. & Bachmann, M. F. Plasmodium vivax malaria vaccines: why are we where we are? *Hum. Vaccin. Immunother.* **9,** 2558–65 (2013).

15. Mota, M. M. *et al.* Migration of Plasmodium sporozoites through cells before infection. *Science* **291,** 141–144 (2001).

16. Lindner, S. E., Miller, J. L. & Kappe, S. H. I. Malaria parasite pre-erythrocytic infection: Preparation meets opportunity. *Cell. Microbiol.* **14,** 316–324 (2012).

17. Baer, K., Klotz, C., Kappe, S. H. I., Schnieder, T. & Frevert, U. Release of hepatic Plasmodium yoelii merozoites into the pulmonary microvasculature. *PLoS Pathog.* **3,** e171 (2007).

18. Bannister, L. & Mitchell, G. The ins, outs and roundabouts of malaria. *Trends Parasitol.* **19,** 209–13 (2003).

19. Baton, L. A. & Ranford-Cartwright, L. C. Spreading the seeds of million-murdering death: metamorphoses of malaria in the mosquito. *Trends Parasitol.* **21,** 573–80 (2005).

20. Okumu, F. O. & Moore, S. J. Combining indoor residual spraying and insecticide-treated nets for malaria control in Africa: a review of possible outcomes and an outline of suggestions for the future. *Malar. J.* **10,** 208 (2011).

21. The malERA Consultative Group on Vector Control. A research agenda for malaria eradication: vector control. *PLoS Med.* **8,** e1000401 (2011).

22. Kondrashin, A. *et al.* Mass primaquine treatment to eliminate vivax malaria: lessons from the past. *Malar. J.* **13,** 51 (2014).

23. Henderson, D. A. Lessons from the eradication campaigns. *Vaccine* **17 Suppl 3,** S53–5 (1999).

24. Malaria Vaccine Funders Group. Malaria Vaccine Technology Roadmap. 1–9 (2013).

25. Vaughan, A. M. & Kappe, S. H. I. Malaria vaccine development: persistent challenges. *Curr. Opin. Immunol.* **24,** 324–31 (2012).

26. Doolan, D. L., Dobaño, C. & Baird, J. K. Acquired immunity to Malaria. *Clin. Microbiol. Rev.* **22,** 13–36 (2009).

27. Nussenzweig, R. S., Vanderberg, J., Most, H. & Orton, C. Protective immunity produced by the injection of x-irradiated sporozoites of plasmodium berghei. *Nature* **216,** 160–162 (1967).

28. Clyde, D. F., Most, H., McCarthy, V. C. & Vanderberg, J. P. Immunization of man against sporozite-induced falciparum malaria. *Am. J. Med. Sci.* **266,** 169–77 (1973).

29. Thera, M. a. & Plowe, C. V. Vaccines for Malaria: How Close Are We? *Annu. Rev. Med.* **63,** 345–357 (2012).

30. Khan, S. M., Janse, C. J., Kappe, S. H. I. & Mikolajczak, S. a. Genetic engineering of attenuated malaria parasites for vaccination. *Curr. Opin. Biotechnol.* **23,** 908–16 (2012).

31. Regules, J. A., Cummings, J. F. & Ockenhouse, C. F. The RTS,S vaccine candidate for malaria. *Expert Rev. Vaccines* **10,** 589–99 (2011).

32. The RTS,S Clinical Trials Partnership . Efficacy and Safety of the RTS,S/AS01 Malaria Vaccine during 18 Months after Vaccination: A Phase 3 Randomized, Controlled Trial in Children and Young Infants at 11 African Sites. *PLoS Med.* **11,** e1001685 (2014).

33. RTS,S Clinical Trials Partnership . Efficacy and safety of RTS , S / AS01 malaria vaccine with or without a booster dose in infants and children in Africa : fi nal results of a phase 3 , individually randomised , controlled trial. Lancet **6736,** (2015).

34. GSK's malaria candidate vaccine, Mosquirix™ (RTS,S), receives positive opinion from European regulators for the prevention of malaria in young children in sub-Saharan Africa | GSK. at <https://www.gsk.com/en-gb/media/press-releases/2015/gsk-s-malaria-candidate-vaccine-mosquirix-rtss-receives-positive-opinion-from-european-regulators-for-the-prevention-of-malaria-in-young-children-in-sub-saharan-africa/>

35. Moorthy, V. S. & Ballou, W. R. Immunological mechanisms underlying protection mediated by RTS,S: a review of the available data. *Malar. J.* **8,** 312 (2009).

36. Crompton, P. D., Pierce, S. K. & Miller, L. H. Advances and challenges in malaria vaccine development. *J. Clin. Invest.* **120,** 4168–78 (2010).

37. Plowe, C. V. in *Infect. Dis. (Auckl).* (ed. P. Kanki and D.J. Grimes) 171–197 (2013).

38. Clyde, D. F. Immunity to falciparum and vivax malaria induced by irradiated sporozoites: a review of the University of Maryland studies, 1971-75. *Bull. World Health Organ.* **68 Suppl,** 9–12 (1990).

39. Cockburn, I. A. *et al.* Prolonged antigen presentation is required for optimal CD8+ T cell responses against malaria liver stage parasites. *PLoS Pathog.* **6,** e1000877 (2010).

40. Hoffman, S. L. *et al.* Protection of humans against malaria by immunization with radiation-attenuated Plasmodium falciparum sporozoites. *J. Infect. Dis.* **185,** 1155–1164 (2002).

41. Schmidt, N. W., Butler, N. S., Badovinac, V. P. & Harty, J. T. Extreme CD8 t cell requirements for anti-malarial liver-stage immunity following immunization with radiation attenuated sporozoites. *PLoS Pathog.* **6,** 1–15 (2010).

42. Hoffman, S. L. *et al.* Development of a metabolically active, non-replicating sporozoite vaccine to prevent Plasmodium falciparum malaria. *Hum. Vaccin.* **6,** 97–106 (2010).

43. Mordmüller, B. *et al.* Direct venous inoculation of Plasmodium falciparum sporozoites for controlled human malaria infection: a dose-finding trial in two centres. *Malar. J.* **14,** 0–10 (2015).

44. Epstein, J. E. *et al.* Live Attenuated Malaria Vaccine Designed to Protect Through Hepatic CD8+ T Cell Immunity. *Science (80-.).* **334,** 475–480 (2011).

45. Seder, R. a. *et al.* Protection Against Malaria by Intravenous Immunization with a Nonreplicating Sporozoite Vaccine. *Science (80-.).* **341,** 1359–1365 (2013).

46. Roestenberg, M. *et al.* Protection against a malaria challenge by sporozoite inoculation. *N. Engl. J. Med.* **361,** 468–477 (2009).

47. Thathy, V. & Ménard, R. Gene targeting in Plasmodium berghei. *Methods Mol. Med.* **72,** 317–31 (2002).

48. Mueller, A.-K. *et al.* Plasmodium liver stage developmental arrest by depletion of a protein at the parasite-host interface. *Proc. Natl. Acad. Sci. U. S. A.* **102,** 3022–3027 (2005).

49. Mueller, A.-K., Labaied, M., Kappe, S. H. I. & Matuschewski, K. Genetically modified Plasmodium parasites as a protective experimental malaria vaccine. *Nature* **433,** 164–7 (2005).

50. Van Dijk, M. R. *et al.* Genetically attenuated, P36p-deficient malarial sporozoites induce protective immunity and apoptosis of infected liver cells. *Proc. Natl. Acad. Sci. U. S. A.* **102,** 12194–12199 (2005).

51. Spring, M. *et al.* First-in-human evaluation of genetically attenuated Plasmodium falciparum sporozoites administered by bite of Anopheles mosquitoes to adult volunteers. *Vaccine* **31,** 4975–4983 (2013).

52. VanBuskirk, K. M. *et al.* Preerythrocytic, live-attenuated Plasmodium falciparum vaccine candidates by design. *Proc. Natl. Acad. Sci. U. S. A.* **106,** 13004–9 (2009).

53. Beaudoin, R. L., Strome, C. P., Mitchell, F. & Tubergen, T. a. Plasmodium berghei: immunization of mice against the ANKA strain using the unaltered sporozoite as an antigen. *Exp. Parasitol.* **42,** 1–5 (1977).

54. Nahrendorf, W. *et al.* Blood-stage immunity to Plasmodium chabaudi malaria following chemoprophylaxis and sporozoite immunization. *Elife* **4,** e05165 (2015).

55. Roestenberg, M. *et al.* Long-term protection against malaria after experimental sporozoite inoculation: An open-label follow-up study. *Lancet* **377,** 1770–1776 (2011).

56. Bijker, E. M. *et al.* Protection against malaria after immunization by chloroquine prophylaxis and sporozoites is mediated by preerythrocytic immunity. *Proc. Natl. Acad. Sci. U. S. A.* **110,** 7862–7 (2013).

57. Zuzarte-Luis, V., Mota, M. M. & Vigário, A. M. Malaria infections: What and how can mice teach us. *J. Immunol. Methods* 1–10 (2014). doi:10.1016/j.jim.2014.05.001

58. Langhorne, J. *et al.* The relevance of non-human primate and rodent malaria models for humans. *Malar. J.* **10,** 23 (2011).

59. Ménard, R. The journey of the malaria sporozoite through its hosts: Two parasite proteins lead the way. *Microbes Infect.* **2,** 633–642 (2000).

60. Coppi, A. *et al.* The malaria circumsporozoite protein has two functional domains, each with distinct roles as sporozoites journey from mosquito to mammalian host. *J. Exp. Med.* **208,** 341–356 (2011).

61. Reyes-sandoval, A. Plasmodium vivax. *Hum. Vaccin. Immunother.* **9,** 2558–2565 (2013).

62. Kumar, K. A. *et al.* The circumsporozoite protein is an immunodominant protective antigen in irradiated sporozoites. *Nature* **444,** 937–940 (2006).

63. Mishra, S. *et al.* Identification of non-CSP antigens bearing CD8 epitopes in mice immunized with irradiated sporozoites. *Vaccine* **29,** 7335–42 (2011).

64. Lin, J. *et al.* A novel 'gene insertion/marker out' (GIMO) method for transgene expression and gene complementation in rodent malaria parasites. *PLoS One* **6,** e29289 (2011).

65. Tewari, R., Spaccapelo, R., Bistoni, F., Holder, A. a. & Crisanti, A. Function of region I and II adhesive motifs of Plasmodium falciparum circumsporozoite protein in sporozoite motility and infectivity. *J. Biol. Chem.* **277,** 47613–47618 (2002).

66. Jacobs-Lorena, V. Y., Mikolajczak, S. A., Labaied, M., Vaughan, A. M. & Kappe, S. H. I. A dispensable Plasmodium locus for stable transgene expression. *Mol. Biochem. Parasitol.* **171,** 40–4 (2010).

67. Nakabayashi, H., Taketa, K., Miyano, K., Yamane, T. & Sato, J. Growth of Human Hepatoma Cell Lines with Differentiated Functions in Chemically Defined Medium Growth of Human Hepatoma Cell Lines with Differentiated Chemically Defined Medium. **42,** 3858–3863 (1982).

68. Nisha Philip, Rachael Orr, and A. P. W. in *Malar. - Methods Protoc.* (ed. Ménard, R.) 99–125 (2013).

69. Ishino, T., Yano, K., Chinzei, Y. & Yuda, M. Cell-passage activity is required for the malarial parasite to cross the liver sinusoidal cell layer. *PLoS Biol.* **2,** E4 (2004).

70. Van Rooijen, N., Sanders, A. & van den Berg, T. K. Apoptosis of macrophages induced by liposome-mediated intracellular delivery of clodronate and propamidine. *J. Immunol. Methods* **193,** 93–9 (1996).

71. Stienstra, R. *et al.* Kupffer cells promote hepatic steatosis via interleukin-1beta-dependent suppression of peroxisome proliferator-activated receptor alpha activity. *Hepatology* **51,** 511–22 (2010).

72. Butler, N. S. *et al.* Superior antimalarial immunity after vaccination with late liver stage-arresting genetically attenuated parasites. *Cell Host Microbe* **9,** 451–462 (2011).

73. Cutts, J. C. *et al.* Immunological markers of Plasmodium vivax exposure and immunity: a systematic review and meta-analysis. *BMC Med.* **12,** 150 (2014).

74. Overstreet, M. G., Cockburn, I. A., Chen, Y.-C. & Zavala, F. Protective CD8 T cells against Plasmodium liver stages: immunobiology of an 'unnatural' immune response. *Immunol. Rev.* **225,** 272–83 (2008).

75. Hoffman, S. L. & Doolan, D. L. Malaria vaccines-targeting infected hepatocytes. *Nat. Med.* **6,** 1218–9 (2000).

76. Doolan, D. L. & Hoffman, S. L. The Complexity of Protective Immunity Against Liver-Stage Malaria. *J. Immunol.* **165,** 1453–1462 (2000).

77. Nganou-Makamdop, K., van Gemert, G.-J., Arens, T., Hermsen, C. C. & Sauerwein, R. W. Long Term Protection after Immunization with P. berghei Sporozoites Correlates with Sustained IFNγ Responses of Hepatic CD8+ Memory T Cells. *PLoS One* **7,** e36508 (2012).

78. Behet, M. C. *et al.* Sporozoite immunization of human volunteers under chemoprophylaxis induces functional antibodies against pre-erythrocytic stages of Plasmodium falciparum. *Malar. J.* **13,** 136 (2014).

79. March, S. *et al.* A microscale human liver platform that supports the hepatic stages of Plasmodium falciparum and vivax. *Cell Host Microbe* **14,** 104–15 (2013).